

H-BRIDGE CONVERTER MODELING AND SIMULATIONS FOR A BATTERY  
POWER MANAGEMENT SYSTEM

By

NASTARAN NIKNAM

Submitted in Partial Fulfillment of the Requirements

for the Degree of

Master of Science

in

Electrical Engineering

YOUNGSTOWN STATE UNIVERSITY

June 2016

# H-Bridge Converter Modeling and Simulations for a Battery Power Management System

Nastaran Niknam

I hereby release this thesis to the public. I understand that this thesis will be made available from the Ohio LINK ETD Center and the Maag Library Circulation Desk for public access. I also authorize the University or other individuals to make copies of this thesis as needed for scholarly research.

Signature:

---

Nastaran Niknam, Student

Date

Approvals:

---

Dr. Frank X. Li, Thesis Advisor

Date

---

Dr. Jalal Jalali, Committee Member

Date

---

Dr. Philip Munro, Committee Member

Date

---

Dr. Salvatore A. Sanders, Dean of Graduate Studies

Date

## Abstract

This thesis presents a power management system with multiple battery cells connected in series. The main focus is to use H-bridge across each battery to manage battery charging and discharging processes. The H-bridge converter charges the batteries and also provides adjustable DC voltage outputs. The multi-cell batteries are connected in series into proposed battery pack. The proposed battery power management system provides load voltage and battery protection, fault diagnostic and battery equalization. In this study, the battery pack of 10 Lithium-Ion cells in series is charged with AC source, a rectifier, and a buck converter. A DC motor is excited by the charger from -37 volt to +37 volt as the load. MATLAB software is used to design and analyze the proposed system.

## Acknowledgment

I would like to express my sincere gratitude to my advisor Dr. Frank X. Li for useful comments, remarks and engagement through the learning process of this master thesis. His guidance helped me in all the time of research and writing of this thesis. I could not imagine having a better advisor and mentor for my research study. His patience and support helped me to overcome my crisis situations and finish this research.

My committee member, Dr Jalal Jalali, who has advised me for the technical details of my research work; I thank him for the systematic guidance and great effort for believing in me. His support and inspiring suggestion have been precious for the development of this thesis content.

My other committee member, Dr. Philip Munro, who motivated me to recover when my steps faltered; I thank him for his support and guidance for my research work.

I would also like to thank my father for his wise counsel and sympathetic ear. The most special thanks go to my husband Sam, who gave me unconditional support and love through all this research work.

## Table of Content

List of Tables.....	vii
List of Figures.....	viii
Chapter 1 Introduction.....	1
1.1 Battery Powered System.....	1
1.2 Research Objectives and Contributions.....	3
1.3 Methodology of Research.....	4
Chapter 2 Battery Stack Modeling with MATLAB.....	5
2.1 Introduction.....	5
2.2 Battery Capacity and Performance.....	6
2.3 MATLAB Simulink Model of a Single Battery.....	7
2.4 MATLAB Simulation of Charging and Discharging of a Single Cell.....	11
Chapter 3 Battery Management System with H-Bridge.....	13
3.1 Overview of a Battery Management System .....	13
3.1.1 Battery Management Systems for Lithium-Ion Cells.....	14
3.2 Battery Management System Design.....	15
3.3 Simulation Results for four Batteries as a Power Source.....	19

Chapter 4 Battery Stack Power Management for a DC Motor.....	23
4.1 Introduction.....	23
4.2 Battery Stack Charging Process Modeling and Simulation.....	24
4.3 DC Motor Characteristics .....	32
4.4 Multilevel Cascaded H-bridge for 10 cells Battery Stack Design .....	43
Chapter 5 Conclusion and Future Work .....	50
Appendix. A .....	51
Reference.....	54

## List of Tables

Table 4.1 Buck-converter parameters.....	28
Table 4.2 Parameter definitions .....	33
Table 4.3 DC motor parameters.....	36

## List of Figures

Figure 1.1: Four cell battery, charged: (a) balanced and (b) unbalanced.....	3
Figure 2.1: The equivalent modified generic battery model .....	9
Figure 2.2: Subsystem of generic battery model in MATLAB.....	10
Figure 2.3: Simulink results of SOC and current and voltage is discharging state.....	12
Figure 2.4: Simulink results of SOC and current and voltage in charging state .....	12
Figure 3.1: Charge shunting with a resistor across cells .....	14
Figure 3.2: The Inverted H-Bridge topology with source .....	15
Figure 3.3: Multiple inverted H-bridge circuits connected in series .....	16
Figure 3.4: Block diagram for battery management system .....	17
Figure 3.5: PWM timing diagram.....	18
Figure 3.6: PWM signal generation.....	18
Figure 3.7: Simulink block for 4 cells Battery Stack .....	20
Figure 3.8: Load voltage.....	21
Figure 3.9: Load current.....	21
Figure 3.10: Battery voltage .....	22
Figure 3.11: Battery current .....	22



Figure 4.1: The block diagram of the system under study.....	23
Figure 4.2: Simulink block of AC-DC rectifier.....	25
Figure 4.3: Input and output voltage of rectifier .....	25
Figure 4.4: Control loop.....	26
Figure 4.5: Buck converter circuit with voltage control feedback.....	27
Figure 4.6: Open- loop simulation block for PI controller design .....	29
Figure 4.7: Battery charger simulation block.....	30
Figure 4.8: Voltage across the battery stack in charging state .....	31
Figure 4.9: Battery charging current.....	31
Figure 4.10: Equivalent circuit of DC motor.....	32
Figure 4.11: Block diagram of DC motor.....	35
Figure 4.12: Block diagram of current and voltage loops.....	35
Figure 4.13: Linearized open loop model in MATLAB .....	36
Figure 4.14: Bode diagram of current open loop transfer function .....	37
Figure 4.15: Pole zero map of open current loop transfer function.....	38
Figure4.16: Bode diagram for updated gain.....	39
Figure 4.17: Margin and phase gains for.....	40

Figure 4.18: Simulink block diagram of DC motor drive in large signal .....	41
Figure 4.19: Reference speed and measured speed of shaft signals.....	42
Figure 4.20: Reference torque and measured torque signals .....	42
Figure 4.21: Battery stacks as variable DC voltage source.....	44
Figure 4.22: Modified battery models in MATLAB Simulink.....	45
Figure 4.23: Multilevel cascaded H bridge converter with generic battery model.....	46
Figure 4.24: Master and slave for multiple level inverter .....	48
Figure 4.25: Battery stack voltage.....	49
Figure 4.26: Load current.....	49

## Chapter 1

### Introduction

#### 1.1 Battery Powered System

In recent years, battery technology has significantly improved. Batteries with smaller size and lighter weight are used in a wide range of products, especially in portable power systems. In battery-powered systems, a battery is used as a main or spare source of energy. Based on the charging power source, the battery stack may have a rectifier to convert AC voltage to DC voltage and a DC-DC chopper to adjust voltage level. Battery powered devices also can supply power for different loads like DC or AC electrical machines. A DC-DC converter is located between charging DC power sources and the battery stack. Battery cell arrangements can be in series or parallel to provide DC charging voltage for the system. Batteries may be connected in other ways to provide high voltage supplies, such as uninterruptable power supply (UPS) in electric utility, solar energy storage [2] and electric vehicle [3, 4].

High voltage batteries can be categorized in different types according to their chemistry such as lithium-ion cells fuel cells and other electrochemical cells. Some batteries are ideal for small projects like household UPS where size is not considered. But for some applications like electric vehicle the size of batteries and their connections as battery stack are main concerns. Most types of rechargeable cells, such as Lithium-Ion cells, should not be discharged below a lower voltage limit or charged above a higher voltage limit. The state operation area (SOA) of Lithium-Ion cells is limited by current,

temperature, and voltage. They will be quickly damaged if overcharged above a certain voltage (4.2 volt). The temperature effects the lifetime of Li-Ion cells which will be drastically reduced if discharged outside a certain temperature range [5, 6]. When a small battery pack with few cells in series is charged, the charging voltage is divided almost equally among the battery cells. However, in electric vehicle applications where a large number of battery cells are connected in series, there is a high possibility that the overall pack voltage is not equally divided among its cells. Consider a three-cell battery pack, charged up to 12.8 volts. As shown in Figure 1.1.a, each cell gets 4.2 volt if the cells are perfectly balanced. Practically, because of production tolerances, uneven temperature distribution and differences in the ageing characteristics of battery cells, there is a possibility that some cells are fully charged and some are partially charged as shown in Figure 1.1. b. In Figure 1.1.b, one cell is overcharged to 5.7 volt which leads to an increase in the battery temperature. In the meantime, the other cells are not fully charged. Cell-balancing techniques can equalize the batteries charge in a battery stack, reduce the cost, control the recharging of battery cells, decrease damage during charging and extend the life of the battery cells.

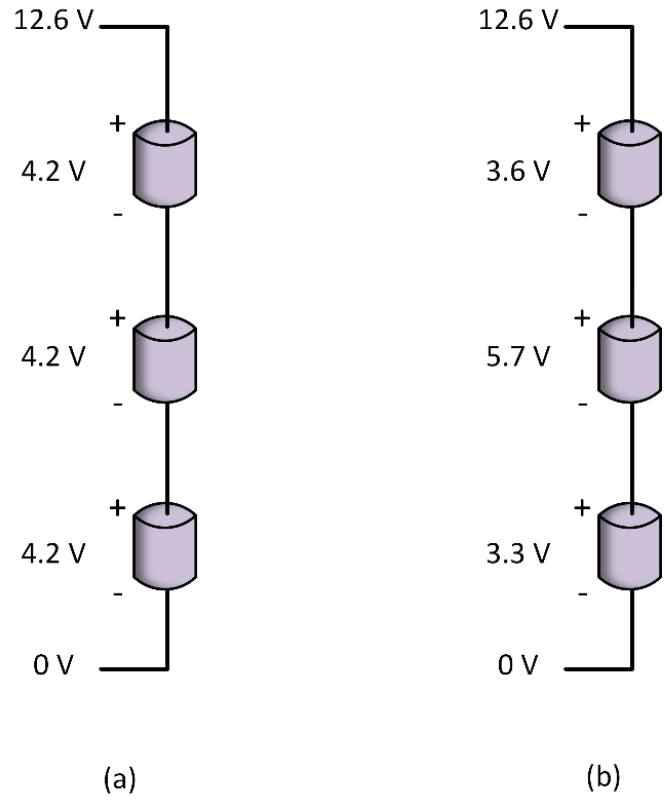


Figure 1.1: Four cells battery: (a) balanced and (b) unbalanced

## 1.2 Research Objectives and Contributions

In this thesis, a combined hardware and software solution to battery power management is used to control the switches across each battery cell. In doing so, the system controls battery charging, balancing, and discharging. This is done by controlling the interconnection scheme of each battery cell with respect to the rest of the cells in the battery pack. By applying this technology to a battery, it becomes a smart battery. In other words, the proposed system is an energy source that is comprised of individual controllable energy storage modules. Each battery cell can be controlled to be in a positive, negative, or bypassed configuration based upon the statuses of the switches.

When a battery fault occurred, the cell can be isolated and bypassed to allow its neighboring cell to continue to function.

### 1.3 Methodology of Research

The research was begun with studies on systems which have a battery stack as their main source of energy. The H-bridge converter capability to handle both battery management and power electronic parts are also investigated. MATLAB is used for modeling and simulating the system. The following tasks have been done in the thesis.

- Task#1: Research for other power management systems for battery-powered power supply in chapter 2.
- Task#2: Investigate H-bridge converter as a part of battery management system in chapter 2.
- Task#3: Proposing a combined hardware and software solution to power management: the software provides the intelligence that controls the hardware, which controls the physical connection among battery cells in chapter 3.
- Task#4: Analyze the feasibility and performance of the proposed controllers via simulation using MATLAB/SIMULINK simulation package in chapter 3.
- Task#5: Design the voltage and current control loops of DC-DC charger with bode-plot method in chapter 4.
- Task#6: Design and analyze of the speed and torque control loops for DC motor control in chapter 4.

## Chapter 2

### Battery Stack Modeling with MATLAB

#### 2.1 Introduction

In this chapter the main characteristics of a battery are discussed. The major components of a battery for modelling are investigated and MATLAB-Simulink model is presented. Battery is a general term for cells that convert stored chemical energy to electrical energy. Batteries may consist of only one cell or may consist of various cells connected to each other. For example, typical 12 V, 40 Ah car batteries have six cells connected in series with the nominal voltage of 2 volt per cell. Batteries can be categorized in different types according to their chemistry compositions such as Lead Acid, Nickel Cadmium, Nickel Hydride and Lithium-Ion. The Lithium-Ion battery is lightest in weight compared to other chemical batteries. The measure of the amount of energy that a battery can hold is referred to energy density. High energy density is one of the largest advantages of Lithium-Ion batteries, which make them compact and small. Nowadays, these batteries are widely adopted in portable electronic devices, such as laptop computers, smart phones and digital cameras. Low maintenance and less self-discharge are other merits of Lithium-Ion battery.

Also, batteries can be categorized in two types according to their recharge abilities. In primary cell, the electrochemical reaction in primary batteries is irreversible after depletion, so the battery is not rechargeable. Primary cells are lighter in weight than secondary cells and suitable for transportation application. Secondary or rechargeable

batteries are more expensive individually; however, they are more cost efficient over a long period of time.

## 2.2 Battery Capacity and Performance

The battery performance depends on many factors such as voltage, electrochemical, temperature, discharge rate etc. One of the most important parameters of the battery known as state of charge (SOC) is the ratio of battery capacity to the nominal battery capacity. SOC shows how much energy has been remained in the battery. The nominal capacity is given by manufacturer and is defined as the maximum capacity that can be stored to the battery. So, the state of charge can be defined as equation (2.1):

$$\text{SOC}(t) = \frac{Q(t)}{Q_n} = \frac{\text{Remaining Capacity}}{\text{Rated Capacity}} \quad (2.1)$$

The equation above is true only at the first cycle of battery life with 100% SOC. The capacity of battery decreases with time as shown in equation (2.2):

$$\text{SOC}(t) = \text{SOC}(0) - \frac{1}{C} \int_0^t I(\tau) d\tau \quad (2.2)$$

Where  $C$  is the nominal capacity of battery in Farad and  $I$  is the cell current in ampere. Temperature is one of the major factors in battery performance. It affects the storage capacity and also the internal resistance of the battery. Usually a good battery temperature range is between 20 and 30 centigrade. Battery life is defined as how long the battery can be expected to perform under ideal conditions. Each battery has limited life, which depends on many factors such as size of battery, manufacturer, capacity and



temperature [11, 12]. Even the unused battery discharges gradually over time because of its self-discharge. Heat is one of the most dangerous factors that make a battery's life shorter. Depth of discharge (DOD) is compliment of state of charge of the battery and it shows how deeply the battery can be discharged. Distracting more energy from a battery makes the cycle life of battery shorter. Full discharge is not recommended in batteries because it shortens the battery life [13].

$$\text{DOD} = 1 - \text{SOC} \quad (2.3)$$

Battery operation varies significantly with age. The ratio of maximum charge capacity of an aged battery to the maximum charge capacity when it is new is defined as state of health of the battery. In other words, the state of health is the battery's ability to deliver power and receive energy. There are two main methods to measure state of health based on measuring full charge capacity FCC and also measuring internal impedance [14].

### 2.3 MATLAB Simulink Model of a Single Battery

There are lots of battery models that represent the behavior of the batteries in many aspects such as battery voltage and current, state of charge and internal resistance .Some of the various available models for a battery are mentioned in this section [15].

In the generic battery model, the process of charging and discharging is the combination of nonlinear and exponential behavior of the battery. This model is easy to use and also can be applied to dynamic simulation software like MATLAB. The generic battery model can represent different chemical batteries behavior including Lithium-Ion, Lead Acid, NiCd Cadmium and NiCd Metal Hydrate accurately. This model consists of a

controlled voltage source and a resistance in series. The internal resistance does not vary with the current extracted from battery and is assumed to be constant. Also the effect of temperature on the battery current, which as described in the Peukert, effect is not considered. The memory effect and self-discharged are also ignored [16]. This model describes the behavior of the battery according to the shepherd equation. The nonlinear term in equation (2.11) indicates that in a fully discharged condition, when the battery current is almost zero and the battery voltage equals to the constant battery voltage. The nonlinear term states how the voltage changes by changing the capacity and the battery current. The equations (2.12) and (2.13) are a modified form of the Shepherd equation and describe the electrochemical behavior of a battery in terms of its voltage, open circuit voltage, internal resistance, discharge current and state of charge. The equation (2.12) and (2.13) refer to the charging and discharging mode. In Figure 2.1, the filtered current and integration of current are provided through low-pass filter and integration blocks. Figure 2.2 shows inside the subsystem of the generic battery model. This block is built according to the charge and discharge equations of Lithium-Ion battery.

$$V_{oc} = E_0 - R_i \cdot i - K \frac{Q}{Q - i} \cdot i \quad \text{Shepherd equation} \quad (2.11)$$

$$V_{dis} = f_1(it, i^*, i) = E_0 - K \frac{Q}{Q - it} \cdot i^* - K \frac{Q}{Q - it} \cdot it + A \cdot e^{(-B \cdot it)} \quad (2.12)$$

$$V_{ch} = f_2(it, i^*, i) = E_0 - K \frac{Q}{0.1 \cdot Q + it} \cdot i^* - K \frac{Q}{Q - it} \cdot it + A \cdot e^{(-B \cdot it)} \quad (2.13)$$

$V_{oc}$ : Open circuit voltage (V)

$i$  : Battery current (A)

$E_0$ : Constant voltage (V)

$B$  : Exponential capacity (Ah)<sup>-1</sup>

$K$ : Polarization coefficient (Ohms)

$Q$  : Battery capacity (Ah)

$i^*$ : Filtered battery current (A)

$i_t$  : Extracted capacity (Ah)

$E_t$ : Terminal voltage of battery (V)

$R_i$ : Internal resistance ( $\Omega$ )

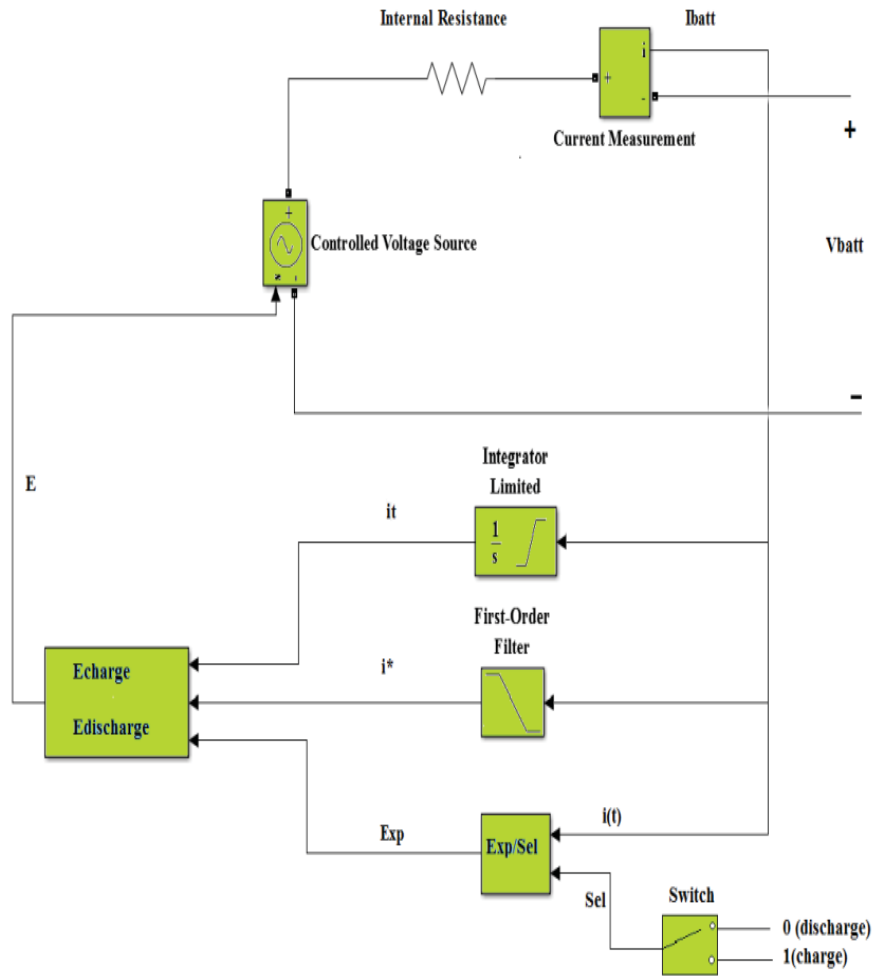


Figure 2.1: The equivalent modified generic battery model

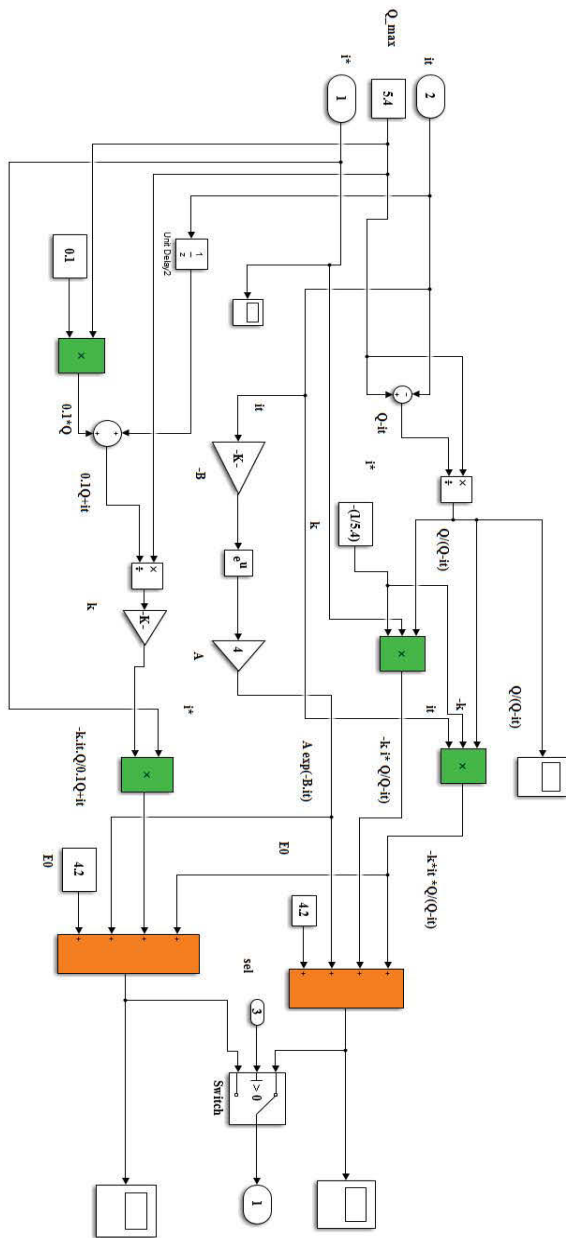


Figure 2.2: Subsystem of generic battery model in MATLAB

## 2.4 MATLAB Simulation of Charging and Discharging Process of a Single Battery

Based on the simulation block shown in Figure 2.3, the charging and discharging plots can be obtained. The maximum capacity of a Lithium Ion battery is assumed to be 5.4 Ah and the rated voltage of a Lithium Ion battery is 4.2 volt. ( $Q_{\max} = 5.4 \text{ Ah}$ ,  $E_{\text{rate}} = 4.2 \text{ V}$ ) Figure 3.3 shows the state of charge, current and voltage of a Lithium Ion battery in discharging state. The upper plot indicates the state of charge is depleted from 100% to zero in 2500 seconds and the bottom plot shows the battery is discharged in less than one hour with 8 A current.

Figure 2.4 shows state of charge, current and voltage of a Lithium-Ion battery in charging state. The upper plot indicates the state of charge increases from 0% to 100% in 7000 seconds and the bottom plot shows the battery is charged in almost two hours with 4 A current.

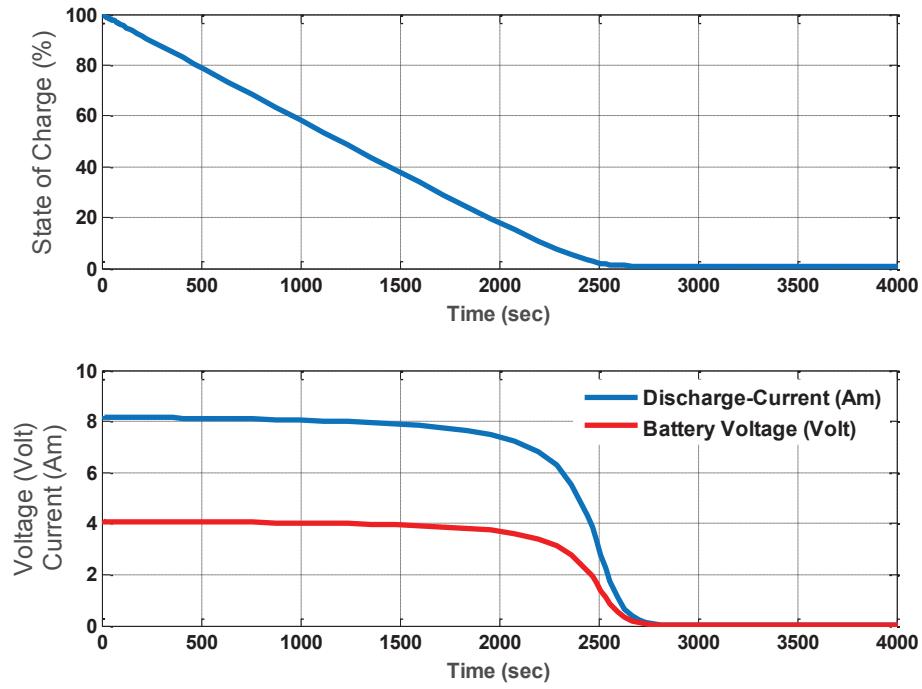


Figure 2.3: Simulink results of SOC and current and voltage in discharging state

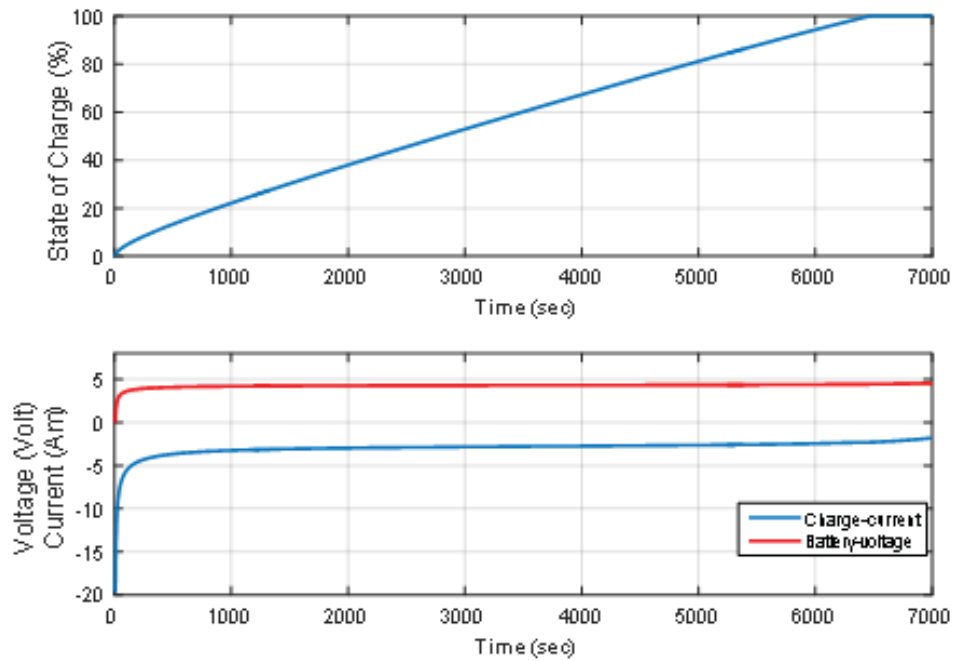


Figure 2.4: Simulink results of state of charge and current and voltage in charging state

## Chapter 3

### Battery Management System with H-Bridge

#### 3.1 Overview of a Battery Management System

The charging process of an individual battery is balanced through a charge equalization strategy named battery management system (BMS), which refers to a hardware configuration employed to achieve the required balancing of cells in terms of state of charge and voltage. Some BMS designs also incorporate a method of communicating data back to a central interface for the user to see or a computer for analysis later. Researchers proposed a design for a BMS with a very clear communication protocol to be transmitted back to a laptop or PC [18]. A general BMS system is presented by balancing cell voltage through DC-DC converters using a central controller [19]. The disadvantage of this system is that there is no communication between batteries and PC or other data logging device to help the user in troubleshooting. Additionally, there is no indication when battery failure has occurred. Usually, a BMS uses a tiny microcontroller to control the switching circuitry for generating various connection configurations. According to the design of the hardware configuration, several charge equalization strategies were developed which are categorized as passive and active charge equalization techniques [20].

##### 3.1.1 Battery Management Systems for Lithium-Ion Cells

There are two types of battery management systems that are commonly found in commercial and industrial lithium battery-based systems. Each type has different benefits

that vary among cost, efficiency, and complexity. Battery stacks that are being used today largely use a passive cell balancing method [21]. The passive system is more basic and it only operates during the charging cycle of the battery stack. A disadvantage of the passive system is that the recovered energy is converted into additional losses in shunt elements [20]. Figure 3.1 shows the passive equalizer with a shunt resistor which is connected across each cell. The resistor can be shunted by switches and each switch is controlled by unit control. The wasting of energy effectively leads to overall lower system efficiency. This method is well suited for systems with small charge current, large power dissipation resistor, and high current switches rise temperature [21].

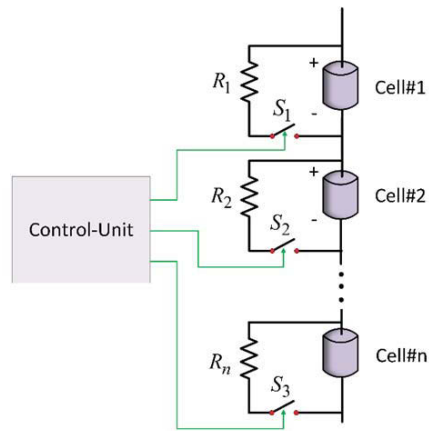


Figure 3.1: Charge shunting with a resistor across cells

The passive balancing technique is used in many applications for their simplicity and lower cost. The active balancing approach is more complex than the passive system. It has the ability to be far more efficient in charging the cells while taking a shorter amount of time. A practical case for a 24V@60Ah battery stack where 6.4 hours and 7.6 were



recorded as a charging time with and without using a balancing system and no balancing system, respectively [23]. In an active balancing BMS, the extra power is used for charging other cells while in a passive system the resistive, power is wasted as heat. The switched capacitor approaches and fly-back converter topology are well-known active techniques that balance the battery cells in many applications [24].

### 3.2 Battery Management System Design

The major contribution of this thesis is to employ a hardware topology that is essentially an “Inverted H-Bridge” as a battery management system. Traditionally, H-bridges have been used to control loads by switches in a given order to provide the load a positive or negative voltage. Each battery cell has its own inverted H-bridge as shown in Figure 3.2 each diagonal pair of switches is linked together. So that the control of the inverted H-bridge only requires 2 control signals. The voltage that appears at input-output terminals I/O port-A and I/O port-B is either; positive  $V_{cell}$ , negative  $V_{cell}$  and zero, where  $V_{cell}$  is the voltage of the cell.

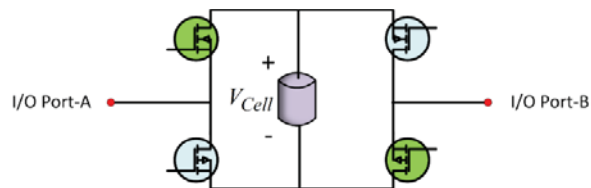


Figure 3.2: The inverted H-Bridge topology with the source

In Figure 3.3 multiple H-bridges are connected in series and a battery pack with a reconfigurable output voltage is created. As a result, this configuration provides the ability to generate AC or DC output and also the battery can be charged with an AC or DC power source.

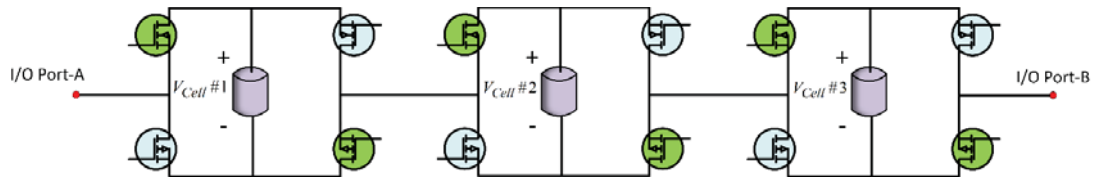


Figure 3.3: Multiple inverted H-bridge circuits connected in series

To generate a desired DC voltage, the cells can be switched in and out at a specified frequency to generate a time averaged voltage equivalent of the desired DC voltage. A passive filter may be employed at this point to smooth out the time averaged DC voltage output.

For implementation of the proposed system we need one master module that is responsible for controlling the slave modules as shown in Figure 3.4. The slave module consists of H-bridge converters. The Master Module receives the cell voltage and current and sends the command signal for controlling the battery stack voltage and protects the faulted or overvoltage battery cell. The number of slave modules may vary from 1 to N depends on application and accessible pins number of microcontroller in master module.

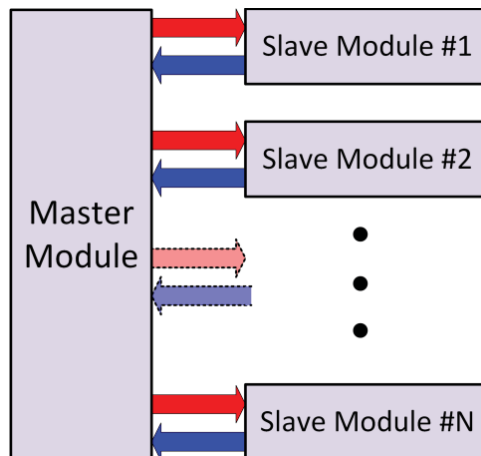


Figure 3.4: Block diagram for battery management system

One of the advantages of the H-bridge converter across each battery is using the Pulse Width Modulation (PWM) technique to generate accurate output voltage. The PWM peripheral works by supplying the correct signal to the H-Bridge. In Figure 3.5, different average output voltages can be adjusted by changing the duty ratio of the control signal. The frequency of the saw tooth signal is switching frequency which is selected based on switch type and output filter. Equation (3.1) defines the duty ratio in respect to the pulse width ( $t$ ) to pulse period ( $T_s$ ). For generating PWM signal, the master block sends the desired voltage signal to the slave blocks. In Figure 3.4, the slave block has two input ports, one is the control signal or the output of master block and the other one is triangular signal to generate PWM signal. Figure 3.6 shows PWM generation signal including the triangular and control waveform. According to equation (3.2) the output average voltage depends on the control voltage, reference voltage and cell voltage.

$$\text{Duty ratio} = D = \frac{\text{Pulse Width}}{\text{Pulse Period}} = \frac{t}{T_s} \quad (3.1)$$

$$V_{\text{out-average}} = \frac{V_c}{V_r} V_{\text{cell}} \quad (3.2)$$

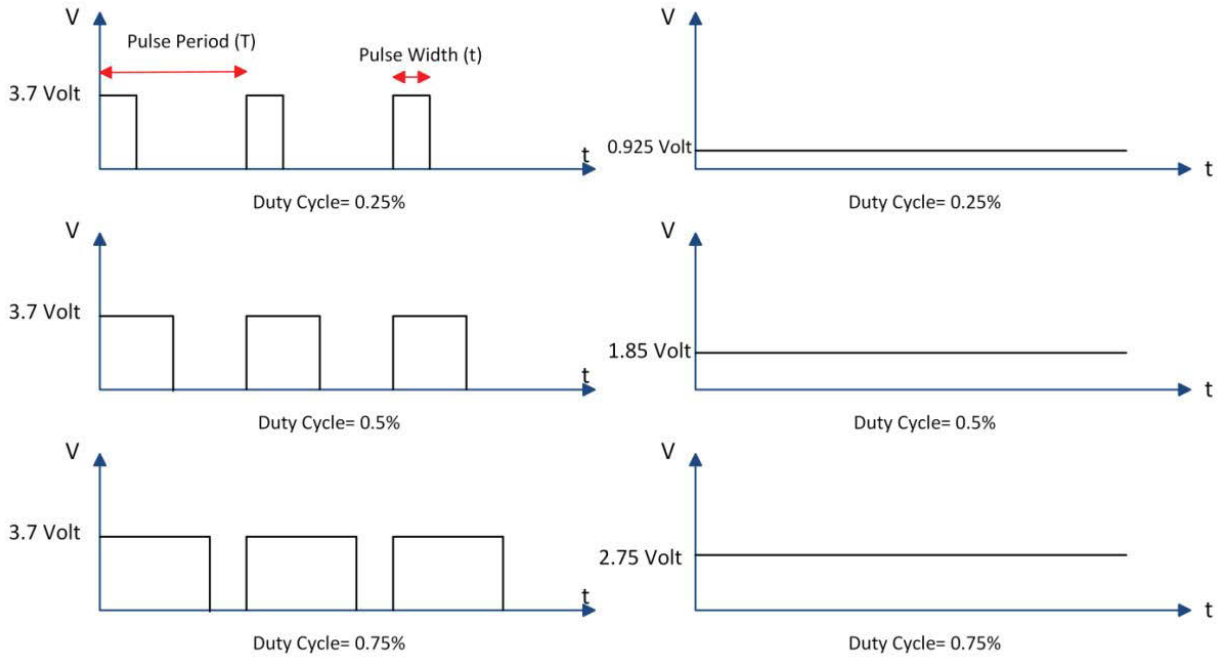


Figure 3.5: PWM timing diagram

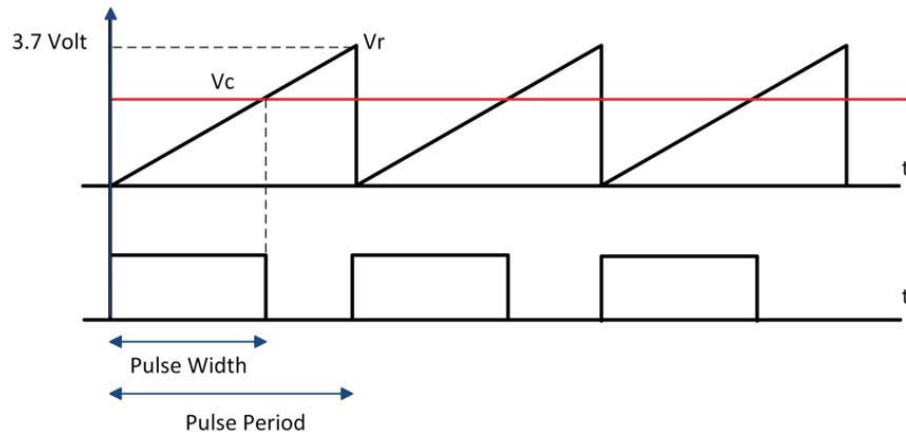


Figure 3.6: PWM signal generation

### 3.3 Simulation Results for four Batteries as a Power Source

In this section the simulation package is presented based on proposed battery management circuit for four batteries which are connected in series. Figure 3.7 shows the simulation blocks consist of a battery stack with 4 H-bridges and RL load. The master

block receives the desired voltage level and sends the control signal to each slave block. The slave block has two inputs as the control signal and the reference signal with 10 KHz frequency as shown in Figure 3.6.

Figure 3.7 shows that the master-slave block is used to produce 9 volt. For generating that level of voltage, two cells completely conduct and one cell produces 1.8 volt by PWM method and one cell is bypassed. Figure 3.8 shows instantaneous load voltage to generate an average 9 volt. The voltage ripples can be diminished by using a capacitor filter. Figure 3.9 shows the total load current from battery cells.

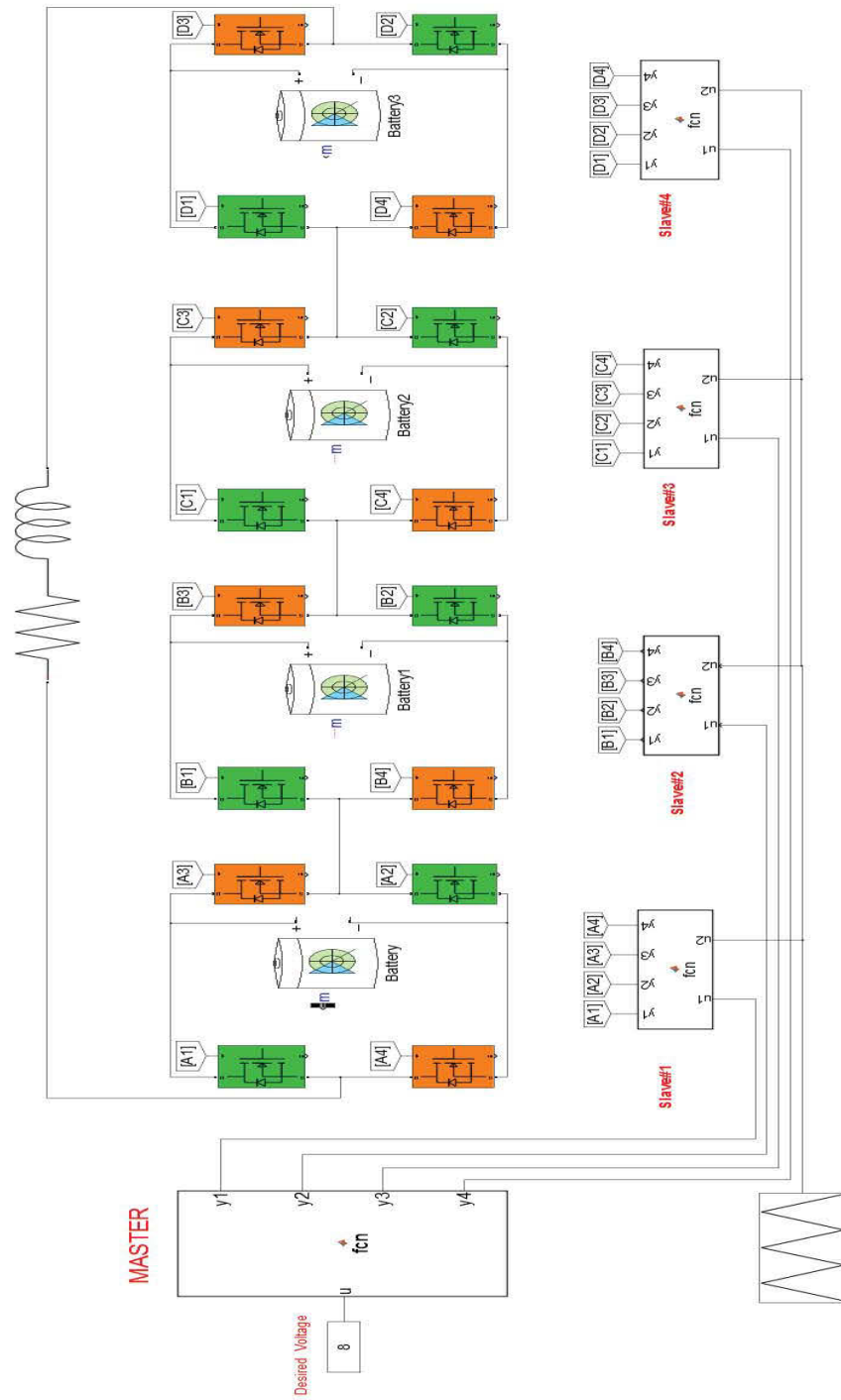


Figure 3.7: Simulink block for 4 cells battery stack

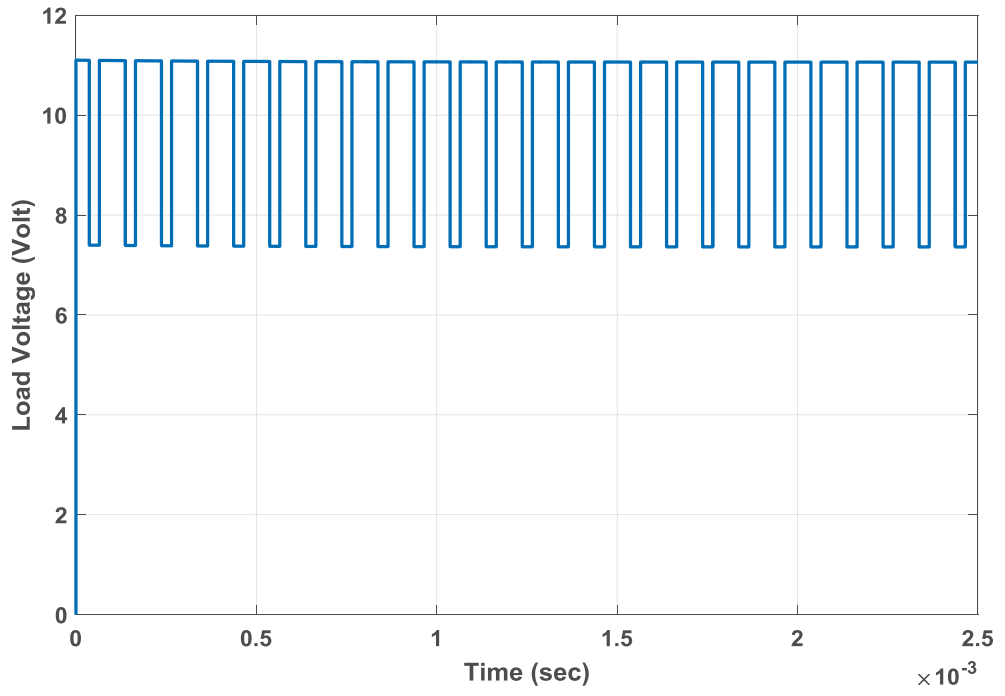


Figure 3.8: Load voltage

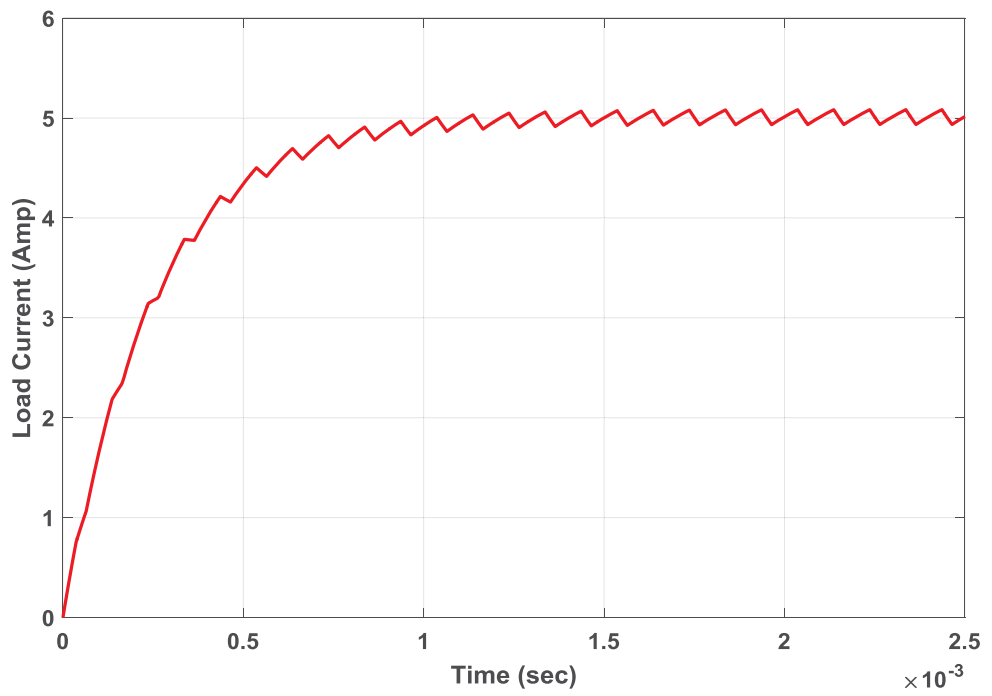


Figure 3.9: Load current

The batteries have 40% SOC and supply voltage is 15 volt. There is a 200  $\mu\text{H}$  inductor between the power supply and battery stack as filter. Figure 3.10 shows the voltage across all batteries and Figure 3.11 shows the charging current with almost 12 amperes.

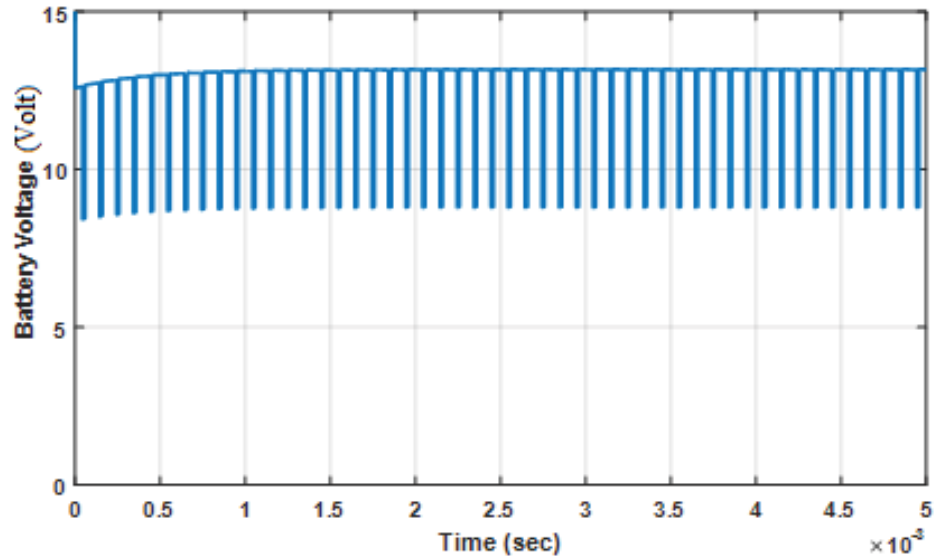


Figure 3.10: Battery voltage

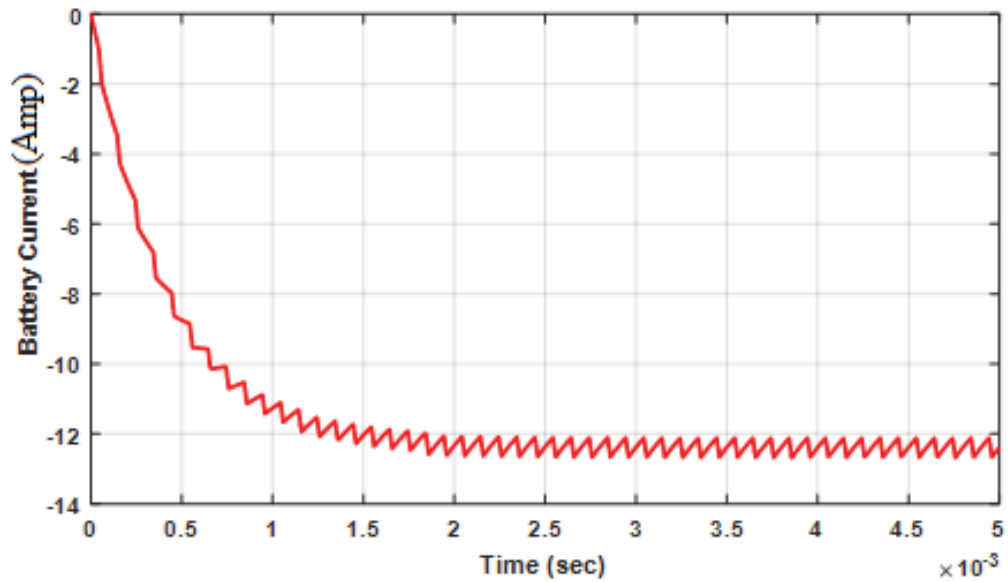


Figure 3.11: Battery current



## Chapter 4

### Battery Stack Power Management for a DC Motor

#### 4.1 Introduction

In this chapter, a practical application of the proposed battery stack is presented. Figure 4.1 shows the block diagram of the entire system of charging and discharging operating modes. The power grid is connected to a linear transformer. The diode bridge rectifier provides DC voltage. The buck converter controls the charging rate to the battery stack with 10 battery cells in series. The separately excited DC motor is employed as a load. During charging the battery stack, circuit breaker 1 (CB#1) is closed and circuit breaker 2 (CB#2) is open and vice versa is true the when DC motor operates. The complete controller design for a DC-DC buck converter and speed control of DC motor are analyzed and discussed through MATLAB simulation. Also, the complete controller design procedure for speed control of DC motor and buck converter are discussed.

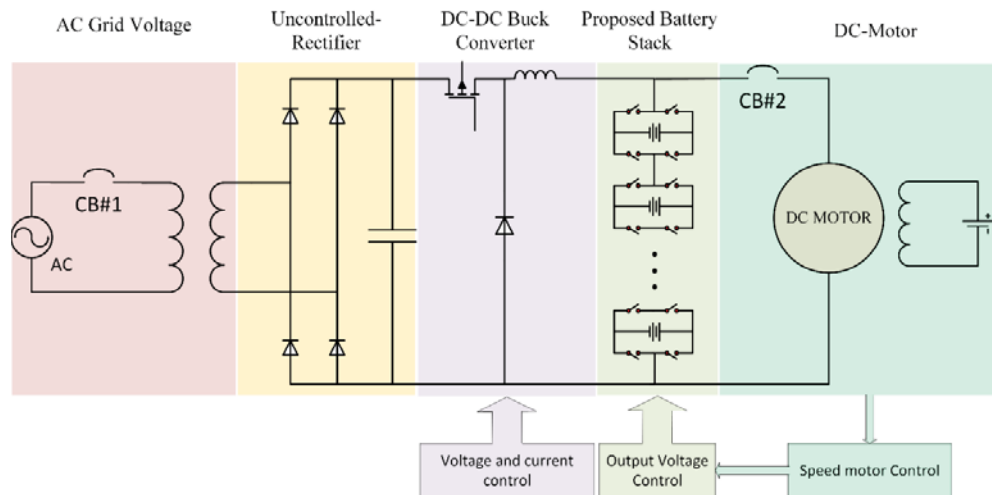


Figure 4.1: The Block diagram of the system under study

## 4.2 Battery Stack Charging Process Modeling and Simulation

In a charging state, the grid voltage is stepped down through a transformer. The purpose of using the transformer is not only to change the voltage level, but also to provide isolation between power mains for safety reason. The ground for two part of transformer is different. The Transformer keeps the circuit from unloading constantly; in the case of a short. An uncontrolled full bridge rectifier is connected to the secondary side of the transformer to convert AC voltage to DC. Equation 4.1 expresses the output voltage for the rectifier.

$$V_o = \frac{2V_m}{\pi} \quad (4.1)$$

Where  $V_m$  is the peak voltage of secondary part of the transformer. The capacitor voltage is used to reduce the ripple in output voltage. In equation (4.2) the output capacitor filter  $C$  can be calculated based on peak to peak ripple  $\Delta V_o$ , grid frequency and resistor during charging state of the batteries.

$$C_f = \frac{V_m}{2fR\Delta V_o} \quad (4.2)$$

In equation (4.3), resistor during the charging state is designed based on the rectifier output voltage and required load current.

$$R = \left(\frac{2V_m}{\pi}\right) / I_{DC-input} \quad (4.3)$$

The output ripple voltage ripple is assumed to be 5% and load current is 10 ampere. Based on these assumptions the output voltage capacitance is 2 mF. Figure 4.2 shows MATLAB Simulink block of the rectifier.

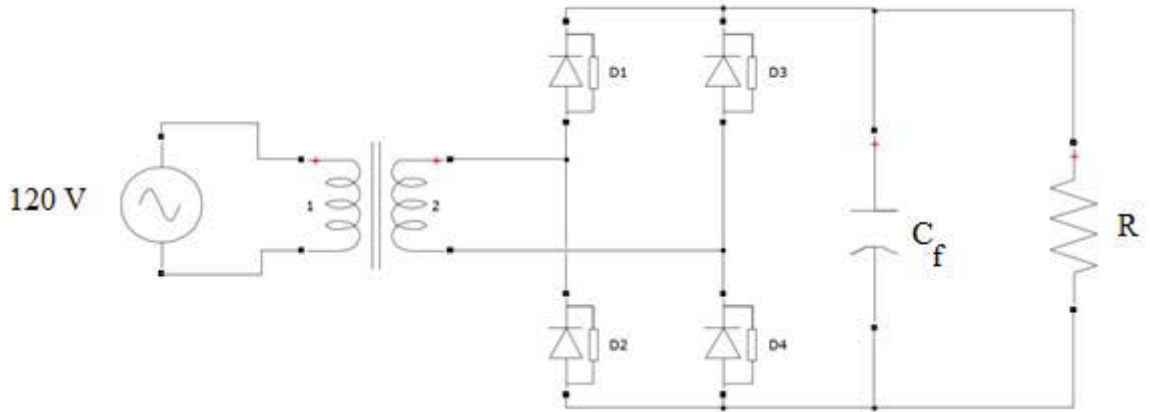


Figure 4.2: Simulink block of AC-DC rectifier

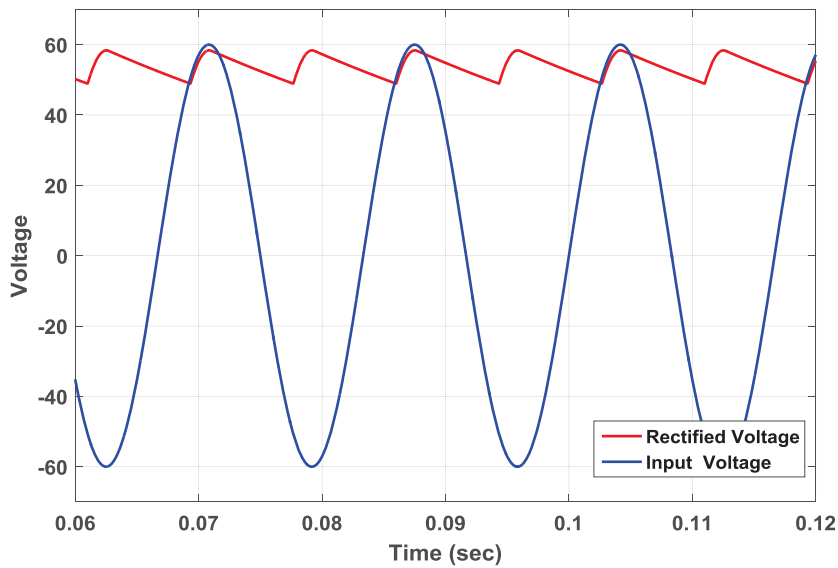


Figure 4.3: Input and output voltage of rectifier

Figure 4.3 shows the output voltage of rectifier which is 60 volt with less than 5% ripple. As expected, the ripple voltage frequency is double the fundamental frequency. In Figure

4.1, the buck converter is used to convert 60 volts DC to the required voltage for batteries to get charged. This section presents the design of a buck converter to regulate the output voltage. The design is based on using voltage mode control. This system is expected to have zero steady state error, fast response and low overshoot.

The design of the battery charger is based on the linear control theory. The main components of the control loop of the buck converter are error amplifier, pulse width modulator, power stage and load as shown in figure 4.4. In the feedback control system, the error between the desired voltage and measured voltage is sent to the PI controller to provide control voltage which is the input of the comparators block. All parts of the feedback control system are linearized around a steady state operating DC point [25].

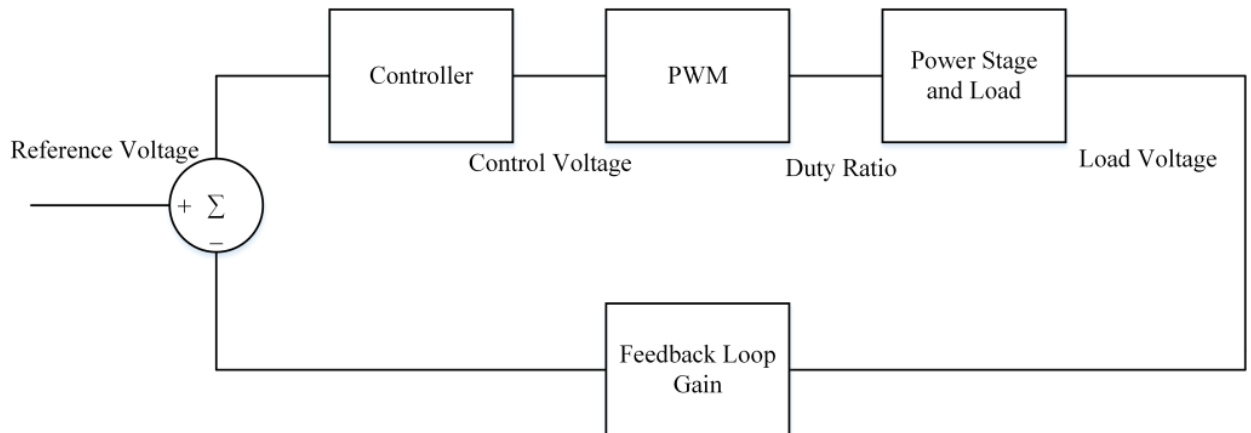


Figure 4.4: Control loop

The disturbance in input voltage or load change leads to variations in the output voltage. The feedback controller is designed to regulate the output voltage. The circuit shown in figure 4.5 is properly designed to automatically adjust the duty cycle “q” to equalize the reference voltage and output measured voltage.

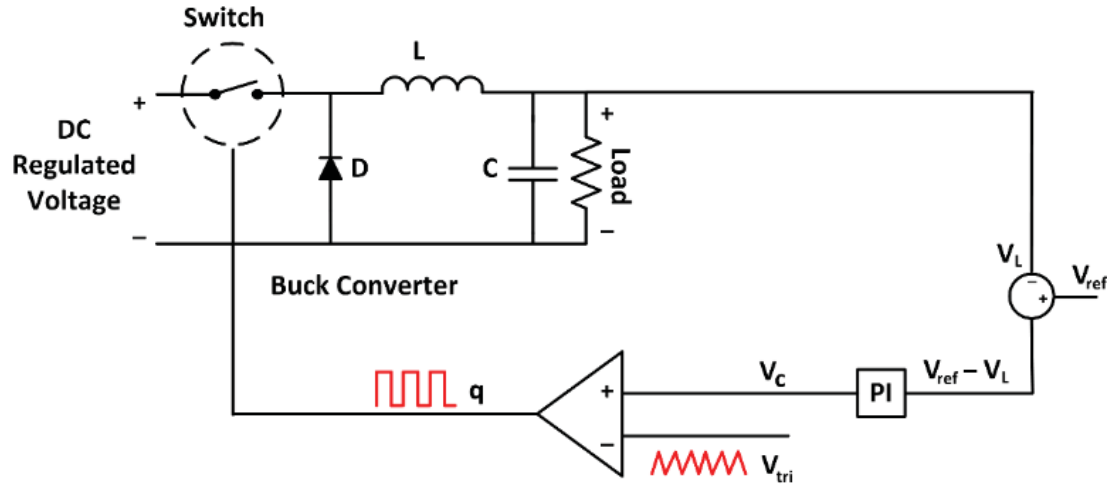


Figure 4.5: Buck converter circuit with voltage control feedback

The first step to design the control system is to model the dynamic behavior of the buck converter. As shown in figure 4.5, the difference between the load voltage and desired voltage (error) acts on the PI controller to generate the control voltage signal. In PWM modulator, the control voltage is compared with triangular waveform to generate the output switching signal.

For designing PI controller, we need a transfer function between the output voltage and duty ratio. This transfer function can be obtained based on average modeling of the system. Equation (4.4) represents the transfer function between output control voltage and duty ratio of buck converter:

$$\frac{\tilde{V}_c(s)}{\tilde{d}(s)} = \frac{V_{in}}{LC} \cdot \frac{1+src}{s^2 + s\left(\frac{1}{RC} + \frac{r}{L}\right) + \frac{1}{LC}} \quad (4.4)$$

The inductor and capacitor of the buck converter are designed based on the desired input current and output voltage ripple, respectively. Table 4.1 shows the buck-converter

parameters. Based on equation 4.4 and Table 4.1, the control loop can be designed with MATLAB simulation.

Table 4.1 Buck-converter parameters

$L$	$100 \mu H$
$r$	$0.1$
$C$	$50 \mu F$
$v_{in}$	$60 V$
$V_{battery-stack}$	$40 V$
$R$	$3.7 Ohm$

The controller parameters are selected based on bode plot method. Figure 4.6 shows the open loop block diagram of the control loop which is used to design PI parameters. Then, open loop frequency responses are used to predict the system behavior in closed loop. For stability reason, there are two rules that should be considered in bode plot method. The gain margin of PI controller should be equal to 1 or in worse situation is -3 db and the phase margin is less than -60 degree.

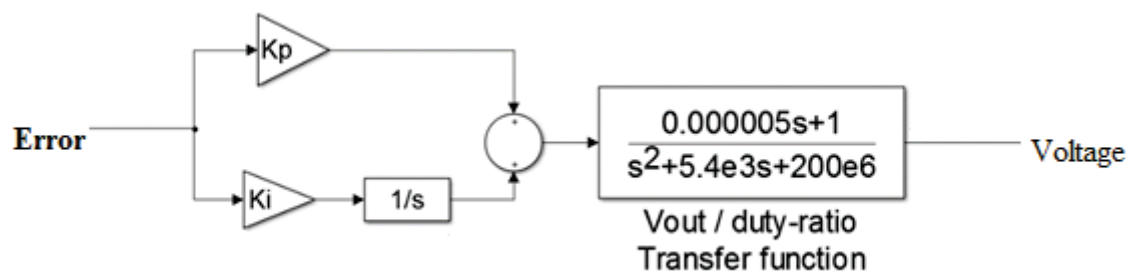


Figure 4.6: Open-loop simulation block for PI controller design

Figure 4.7 shows the power stage simulation blocks of rectifier and DC-DC converter and the battery stack. The load voltage is measured and compared with reference voltage; the error is passed through a PI controller to produce the control voltage. The control voltage is compared with 50 kHz triangular waveform to give PWM signal which is applied to the switch.

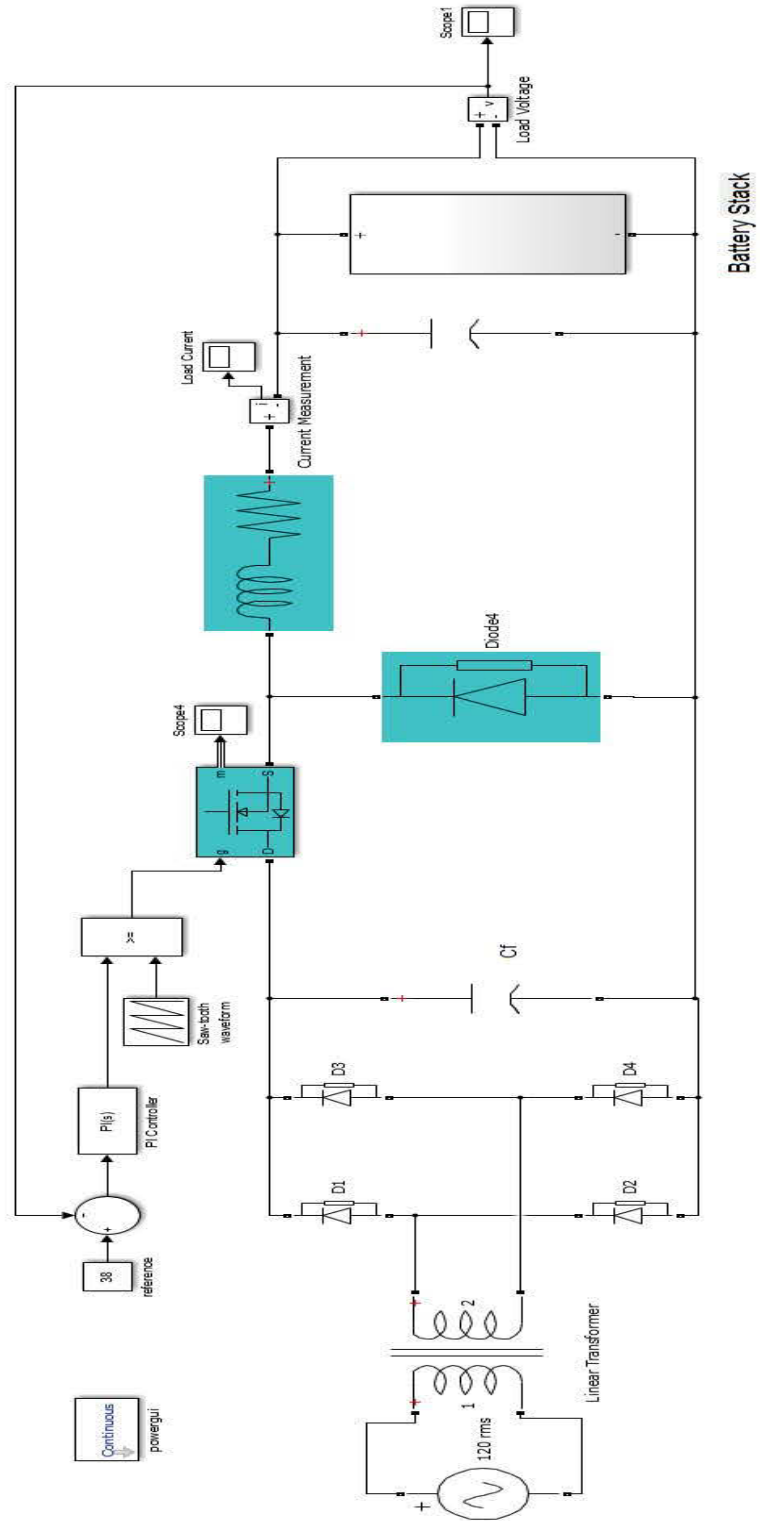


Figure 4.7: Battery charger simulation block



Figure 4.8 shows the voltage across the battery stack. Figure 4.9 shows the battery current which is almost 5 ampere with small ripples. Current ripple can be determined based on inductor selection [1]. The acceptable ripple is less than 5 percent and this design meet the requirement which is 4 percent.

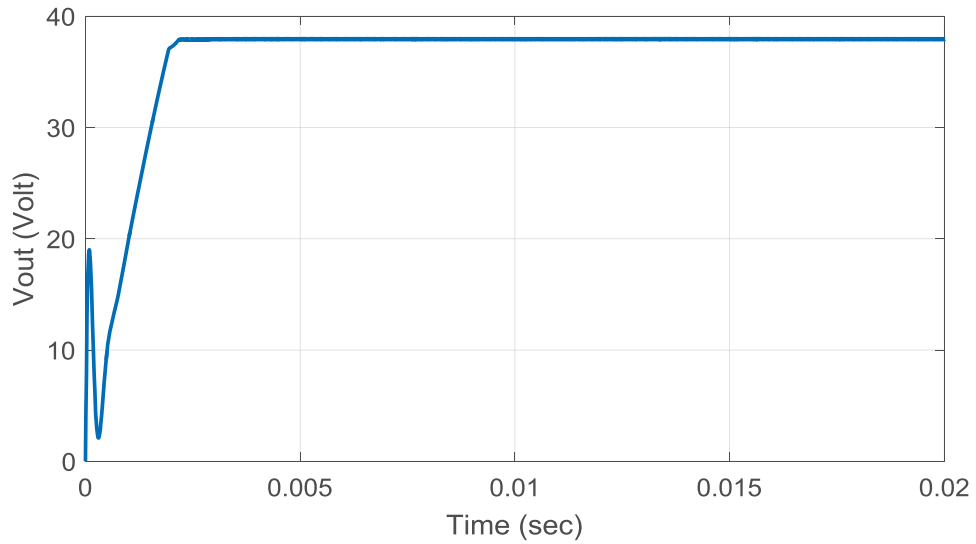


Figure 4.8: Voltage across the battery stack in charging state

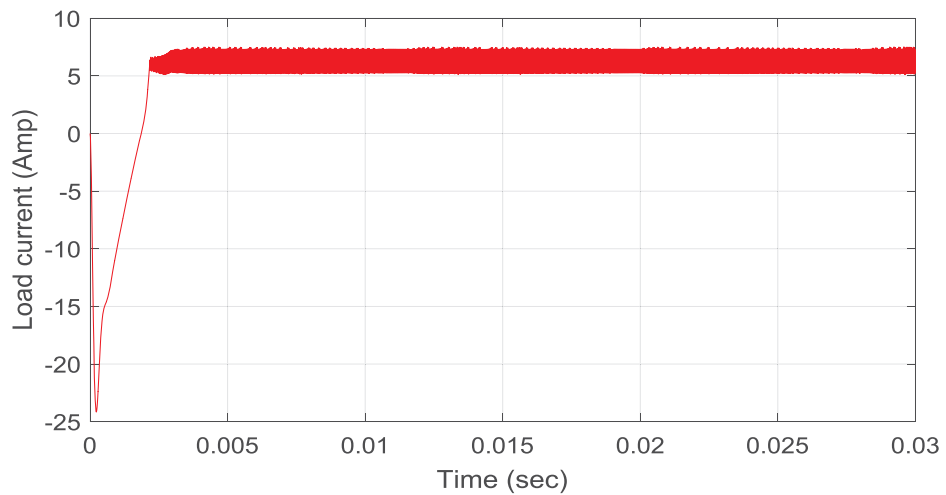


Figure 4.9: Battery charging current

### 4.3 DC Motor Characteristics

DC motors are used where high torque and variable speed is required. They offer a wide range of speed control from zero to the base speed. The DC motor construction is based on the interaction of an electromagnetic field in rotor and stator. The stator or fixed part provides the constant magnetic field. The armature or rotating part is connected to a DC source through commutator rings. When supplied electric current in a commutator passes through the coils, an electromagnetic force is induced on it according to the Lorentz law and the coil starts to rotate.

In this thesis, a separately excited DC motor is selected as a load for the battery stack. In this motor the field circuit is supplied from separated DC source. Figure 4.9 shows the block diagram of a typical DC motor. Speed control with armature voltage control method will be discussed later. A DC motor has two distinct circuits: field circuit and armature circuit.

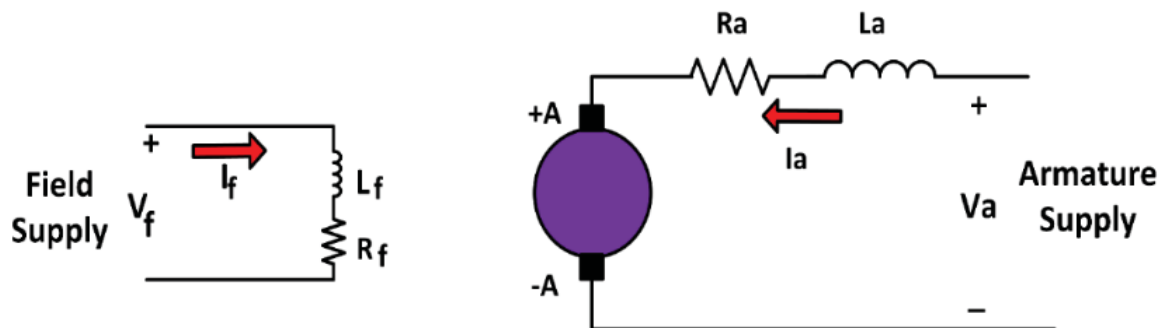


Figure 4.10: Equivalent circuit of DC motor

Applying KVL in the armature and field loops leads to equation (4.5) and equation (4.6).

Equation (4.7) represents that the induced voltage in armature depends on flux and the

speed of motor. Also electromagnetic torque in DC motor is obtained from equation 4.8.

Table 4.2 explains the parameter definitions used in the above equations.

$$V_a = R_a i_a + L_a \frac{di_a}{dt} + e_a \quad (4.5)$$

$$V_f = R_f i_f + L \frac{di_f}{dt} \quad (4.6)$$

$$e_a = K_E \phi \omega \quad (4.7)$$

$$T_e = K_t \phi i_a \quad (4.8)$$

$$\omega = \frac{e_a}{K_E \phi} \rightarrow \omega = \frac{V_a - R_a I_a}{K_E \phi} \quad (4.9)$$

$$\omega = \frac{V_a}{K_t \phi} - \frac{R_a T_e}{(K_t \phi)^2} \quad (4.10)$$

Table 4.2: Parameter definitions

$R_a$ : Armature winding resistance (Ohms)	$V_f$ : Field voltage (V)
$R_f$ : Field winding resistance (Ohms)	$V_a$ : Armature voltage (V)
$e_a$ : Electromotive force of armature (V)	$w$ : Shaft speed (RPM)
$K_E$ : constant motor voltage (volt-sec/rad)	$T_e$ : Electrical torque (Nm)
$L_a$ : Armature winding inductance (H)	$K_t$ : Constant motor torque (Nm/A)
$i_a$ : Armature current (A)	$i_f$ : Field current (A)

According to the equation (4.10), the motor speed can be changed by making any changes in armature voltage, field flux or armature resistance. Also, it shows by increasing the armature voltage the motor speed will be increased and vice versa. In this

thesis, the “armature voltage technique” is used to control the DC motor speed. In this method, the resistance of the armature and flux are constant. Laplace transformation can be used to simplify an electrical system to a model with mathematical equations. Following equations are Laplace forms of DC motor equations.

$$V_a = R_a I_a + E_a + sL_a I_a \quad (4.11)$$

$$V_a - E_a = (R_a + sL_a) I_a \quad (4.12)$$

$$I_a = \frac{V_a - E_a}{R_a + sL_a} \quad (4.13)$$

$$E_a = K_E \phi \omega \quad (4.14)$$

$$T_E = K_T \phi I_a \quad (4.15)$$

$$T_E - T_L = (J s + B) \omega \quad (4.16)$$

Using the above equations, the dynamic of a DC motor can be modeled. Figure 4.10 shows the dynamic block diagram representation of a DC motor. With this figure, the transfer function between motor speed and applied voltage can be obtained easily.

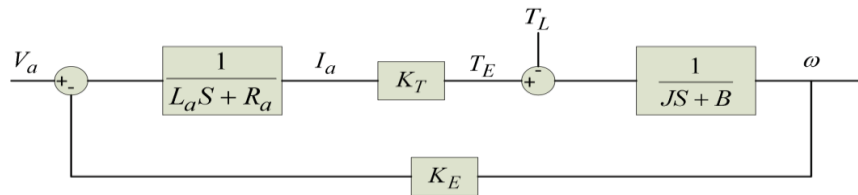


Figure 4.11: Block diagram of DC motor

The motor speed is controlled by a feedback system known as a speed control loop and current control loop. As shown in Figure 4.11, in the outer loop the shaft speed is sensed and compared with reference speed, the speed controller provides referenced torque. In

the inner loop, the motor current is measured and converted to actual torque using constant torque coefficient  $k_t$ . The torque controller generates the required duty ratio for the converter. The output of the converter is the proper voltage to control the shaft speed.

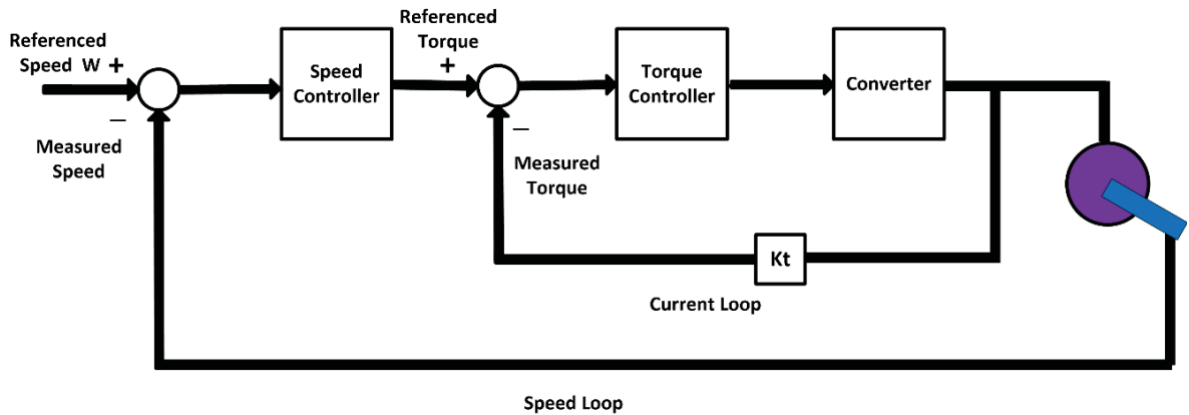


Figure 4.12: Block diagram of current and voltage loops

Table 4.3 represents the parameters for a typical DC motor. Based on the DC motor parameters and Laplace equations, the transfer function of the shaft speed to the motor voltage can be calculated.

Table 4.3 DC motor parameters

Armature resistance	$R_a = 2 \Omega$
Armature inductance	$L_a = 5.2 \text{ mH}$
Shaft inertia	$J_{eq} = 152 \times 10^{-6} \text{ kg} \cdot \text{m}^2$
Friction coefficient	$B = 10 \times 10^{-6} \text{ nm}/\text{rad} \cdot \text{s}^{-1}$
DC-bus voltage	$V_{dc} = 60 \text{ V}$
Torque coefficient	$K_T = 0.1 \text{ nm}/\text{A}$
Back-EMF coefficient	$K_E = 0.1 \text{ V}/\text{rad} \cdot \text{s}$
Triangular peak voltage	$V_{tri} = 5 \text{ V}$
Switching frequency	$f = 33 \text{ KHz}$
Rated speed	$N = 1000 \text{ rpm}$

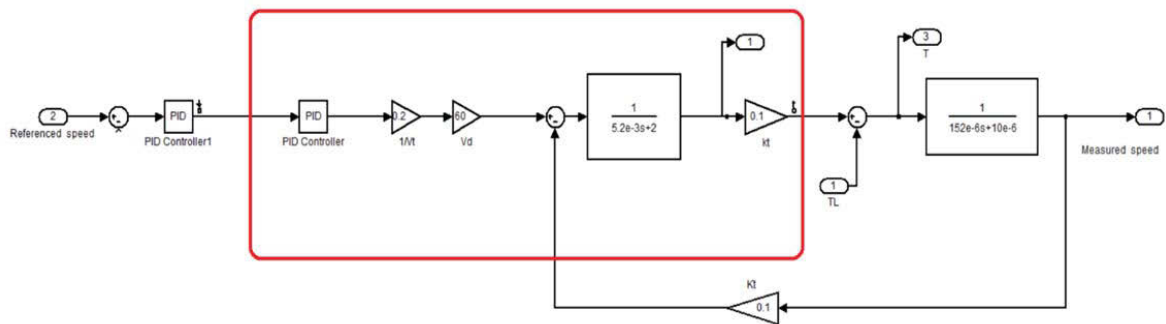


Figure 4.13: Linearized open loop model in MATLAB

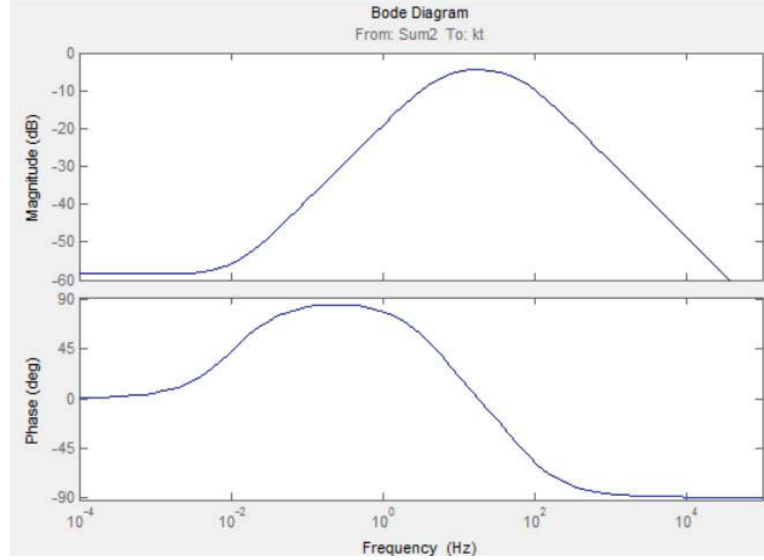


Figure 4.14: Bode diagram of current open loop transfer function

Figure 4.13 shows the MATLAB Simulink block of linearized open loop model. The PI controller design starts from the inner loop. Figure 4.14 shows a bode-plot diagram of current loop transfer function without PI controller ( $K_p=1$ ,  $K_i=0$ ). The bandwidth of the current loop is one order lower than the switching frequency (33 KHz). So the bandwidth of current loop is 3.3 KHz. According to the bode diagram, the magnitude of transfer function is not equal to 1 (0 dB) at 3.3 KHz. The location of  $K_p$  and  $K_i$  can be obtained from pole zero diagram. Figure 4.14 shows the pole zero diagrams for the current loop. It shows this system has two poles and one zero in  $P_1 = -36.4$   $P_2 = -348$   $Z = -0.0658$ . So, the transfer function for current loop  $G_o$  can be obtained from equation (4.24).

$$G_o = \frac{K(s + 0.0658)}{(s + 36.4)(s + 348)} \quad (4.24)$$

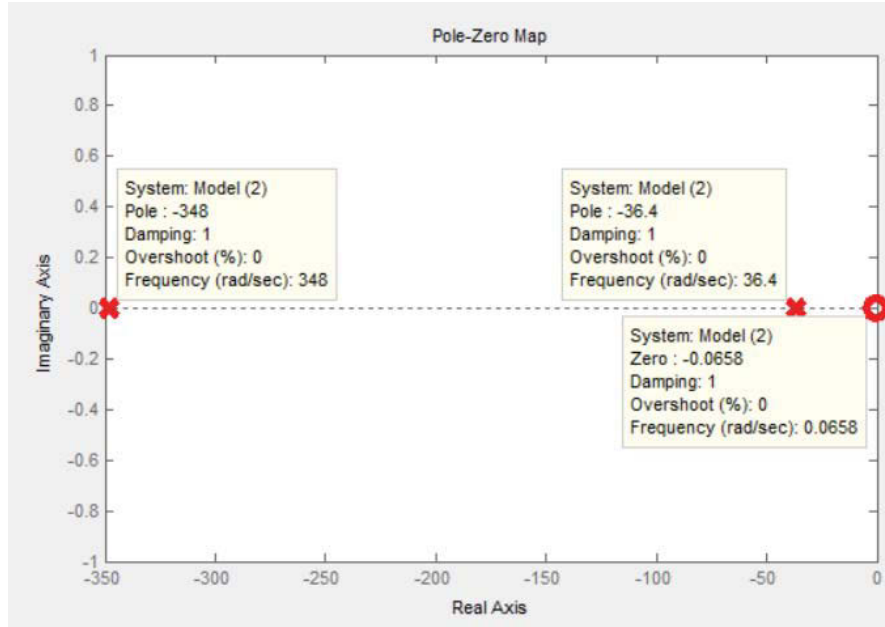


Figure 4.15: Pole zero map of open current loop transfer function

Current PI components are selected to compensate the required magnitude of the current loop. It means the PI components should be selected in a way that the desired phase margin and bandwidth can be obtained. For any system the PI controller can be written in the following equation form:

$$G_{PI} = K_P + \frac{K_i}{s} = K_i \frac{(s/\left(\frac{k_i}{k_p}\right) + 1)}{s} \quad (4.25)$$

According to equation (4.26) in PI controller the gain margin is expected to be zero db from very low frequency to the bandwidth.

$$\frac{(s+0.0658)}{(s+36.4)(s+348)} \times \frac{(s/\left(\frac{k_i}{k_p}\right)+1)}{s} = 1 \quad (4.26)$$



Open loop frequency response re-plotted with  $K_i = 1$   $K_p = 1/200$  in Figure 4.15. The zero of the PI controller should be between two poles of open loop transfer function ( $G_o$ ). By choosing  $K_i = 1$   $K_p = 1/200$ , the new bode-plot is obtained as shown in figure 4.15. The blue color in figure 4.16 is open loop frequency response.

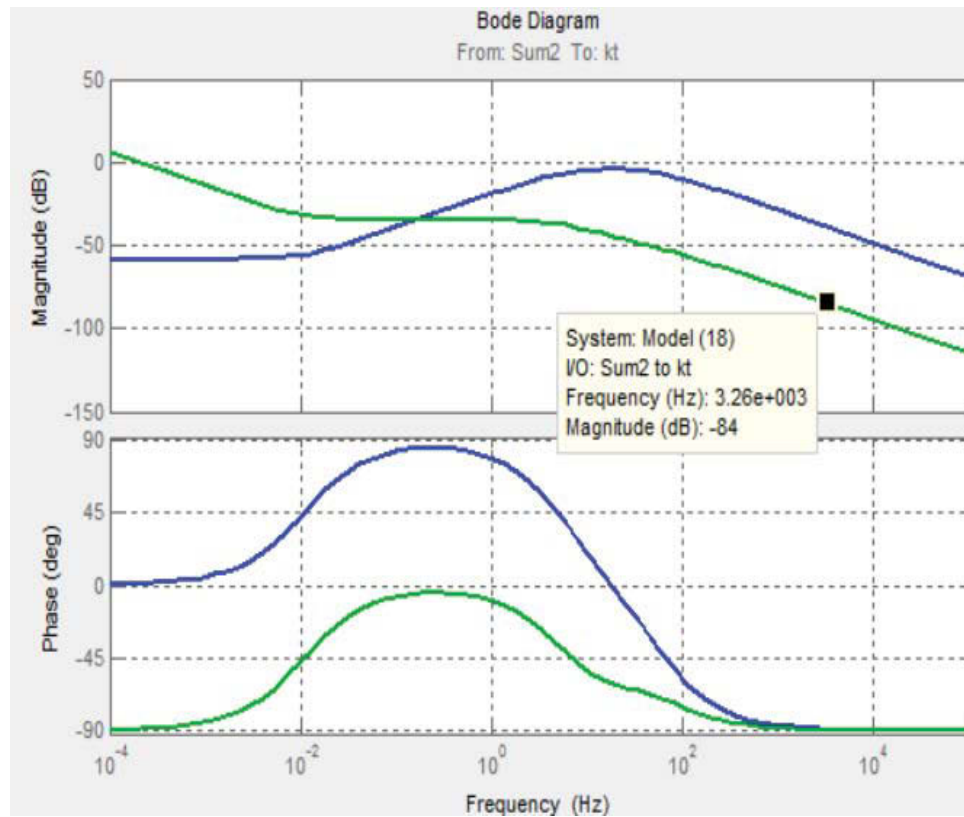


Figure 4.16: Bode diagram for  $K_i = 1$   $K_p = 1/200$

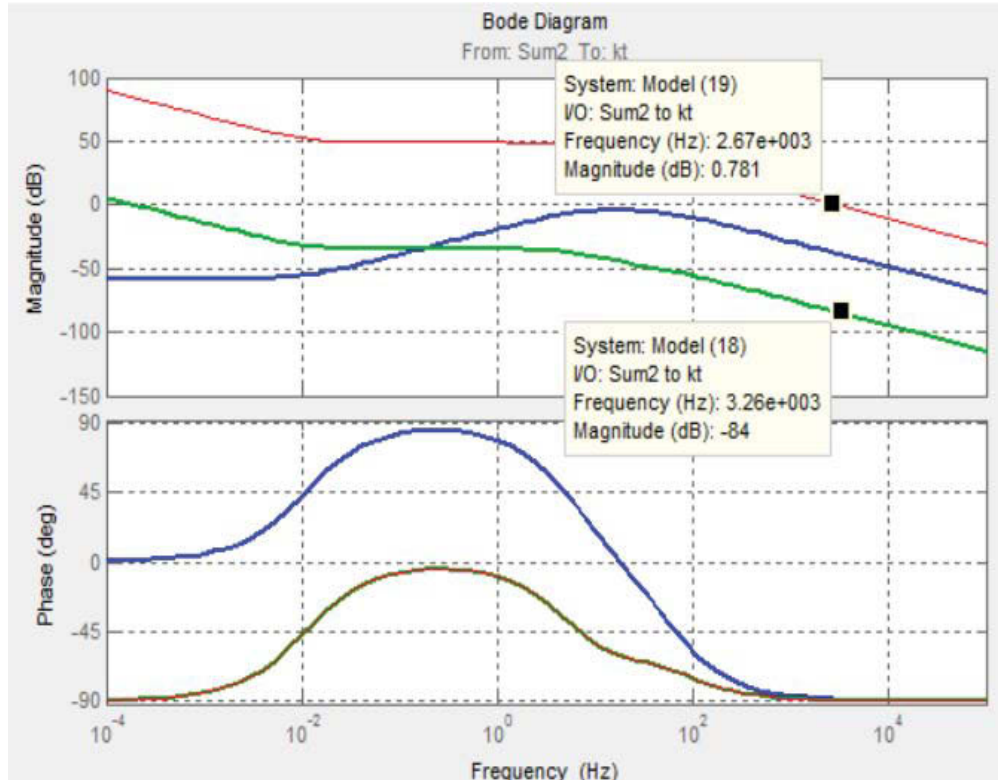


Figure 4.17: Margin and phase gains for  $K_i = 1$   $K_p = 1/200$

For increasing the magnitude of gain in figure 4.16,  $K_i$  can be changed to get the desired magnitude in specified frequency. A new bode diagram with updated PI components is shown in figure 4.16. It shows that magnitude is almost zero at  $f = 3.3$  KHz . With a transfer function for the torque PI controller, the speed PI controller can be designed. The same procedure is used to find speed loop PI components. The final value for the components of torque and speed PI controller are listed as follows:

Torque Control	$K_p = 42$	$K_i = 89000$	$PI = 42 + \frac{89000}{s}$
Speed Control	$K_p = 0.042$	$K_i = 0.6$	$PI = 0.042 + \frac{0.6}{s}$

Based on designed PI parameters, the large signal model for DC motor drive is simulated in MATLAB as shown in Figure 4.17. The battery stack receives the required voltage from output of a second PI (Torque controller). The signal generator is the square wave with the amplitude of 30 volt and 5 Hertz frequency. It is expected that with a good PI controller design DC motor speed tracks the signal generator voltage. DC motor speed is compared to this signal and the difference is sent to the PID. The saturation block bounds the range of an input signal to upper and lower saturation values. The upper and lower limit is  $\pm 0.5$  volt. The inner PID compares the reference torque with the measured torque.

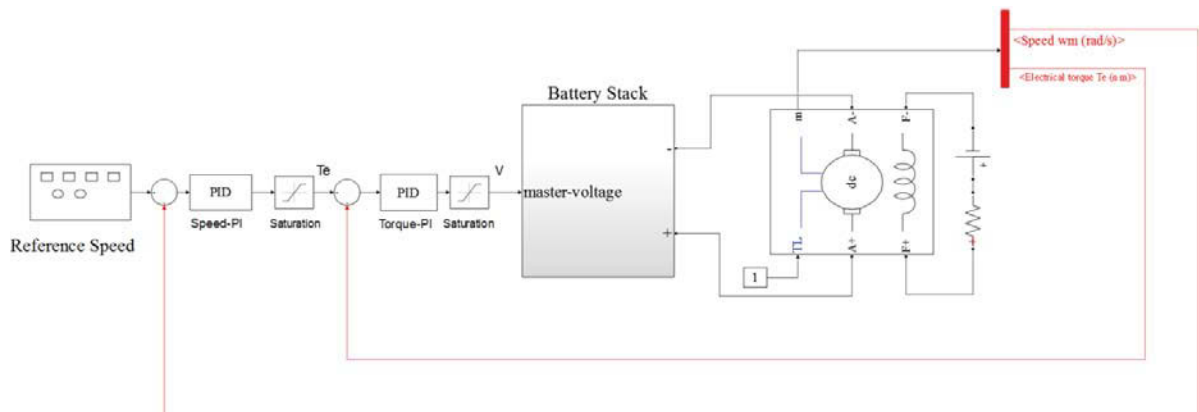


Figure 4.18: Simulink block diagram of DC motor drive in large signal

The shaft speed is measured and compared to the reference speed. The reference speed signal is assumed to be a square signal with 5 KHz frequency and 30 volts amplitude. The result is shown in Figure 4.18. The response for speed is 0.19 seconds. The output of speed PI is the referenced torque which is compared to the actual torque and the

difference acts on the torque PI. The result is shown in Figure 4.19. In this figure, the yellow line which has more distortion is measured torque and the pink line is reference signal.

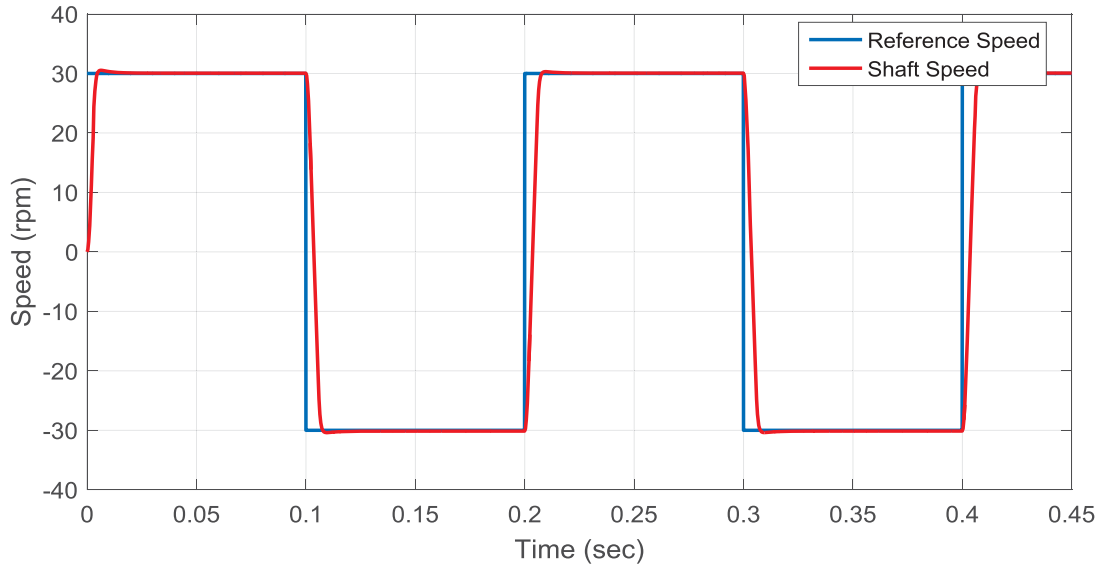


Figure 4.19: Reference speed and measured speed of shaft signals

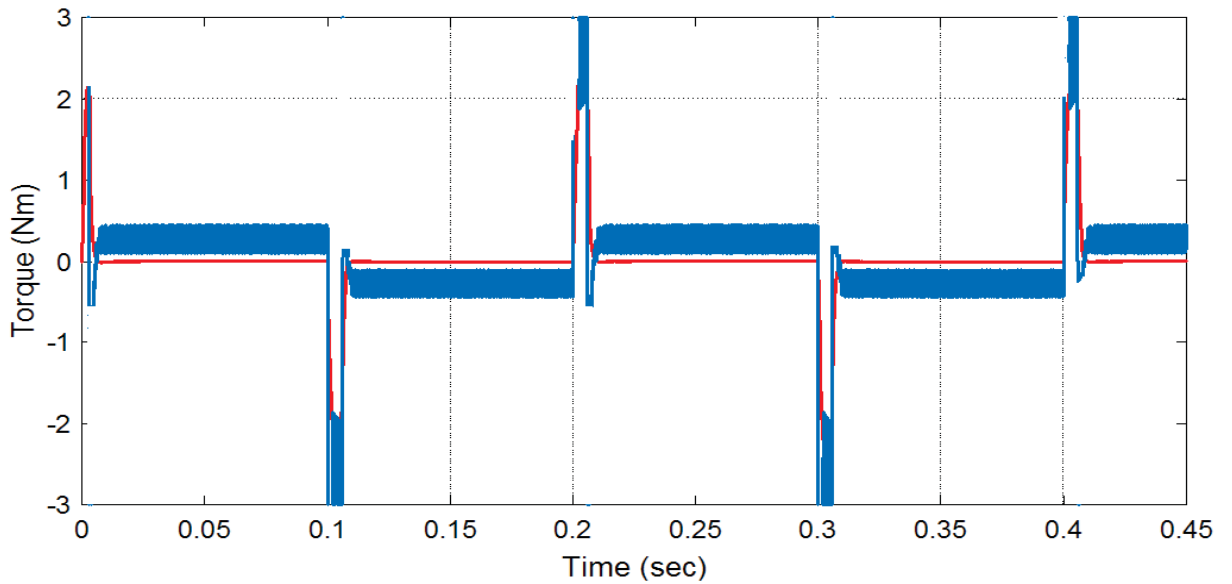


Figure 4.20: Reference torque and measured torque signals

#### 4.4 Multilevel Cascaded H-bridge for 10 cells Battery Stack Design

Figure 4.20 shows the Simulink block of 10 H-bridges with batteries as DC sources. H-bridges are connected by batteries with equal voltage of 3.7 volts. For each H-bridge different combinations of four MOSFET switching states generate three different voltage levels:  $\pm 3.7, 0$  V. Therefore, 10 batteries in the circuit with 40 MOSFET switches generate 21 different voltage levels. In Figure 4.25 the green switches and blue switches works complementary. The load resistance equals to  $2 \Omega$  and load inductance is 5.2 mH. The batteries are substituted with a modified generic battery model in Figure 4.21. The battery is modeled with the modified generic model can be concluded with subsystem in Figure 4.22.

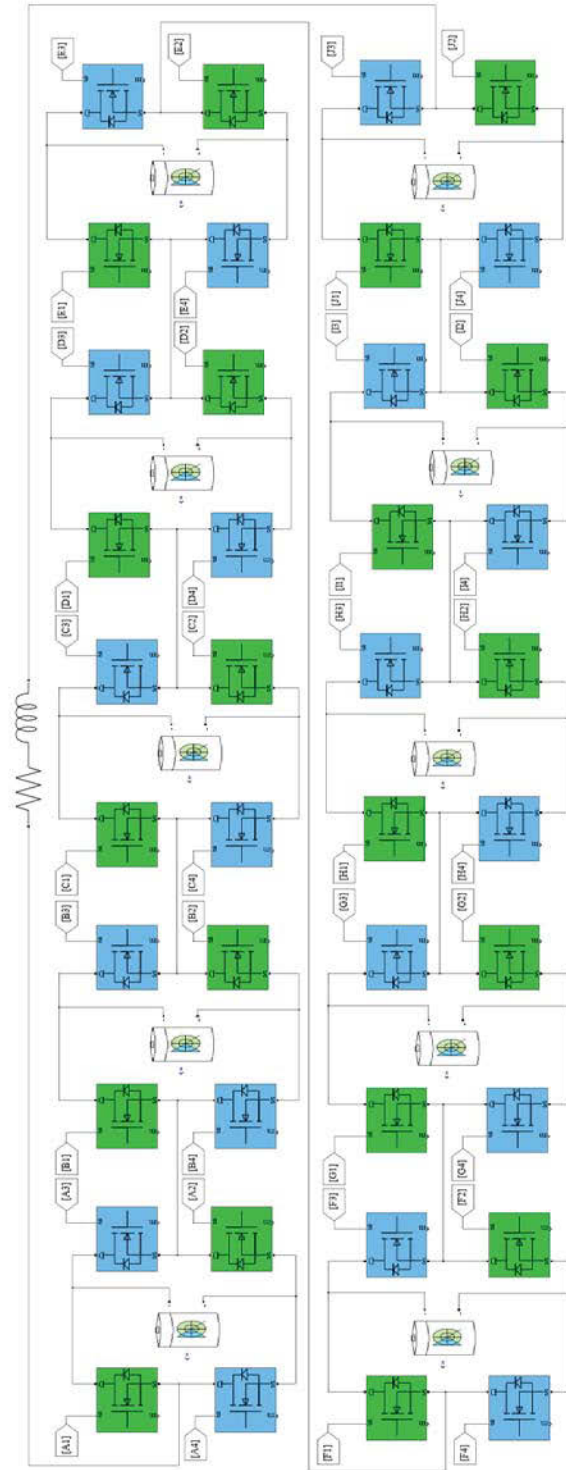


Figure 4.21: Battery stacks as variable DC voltage source

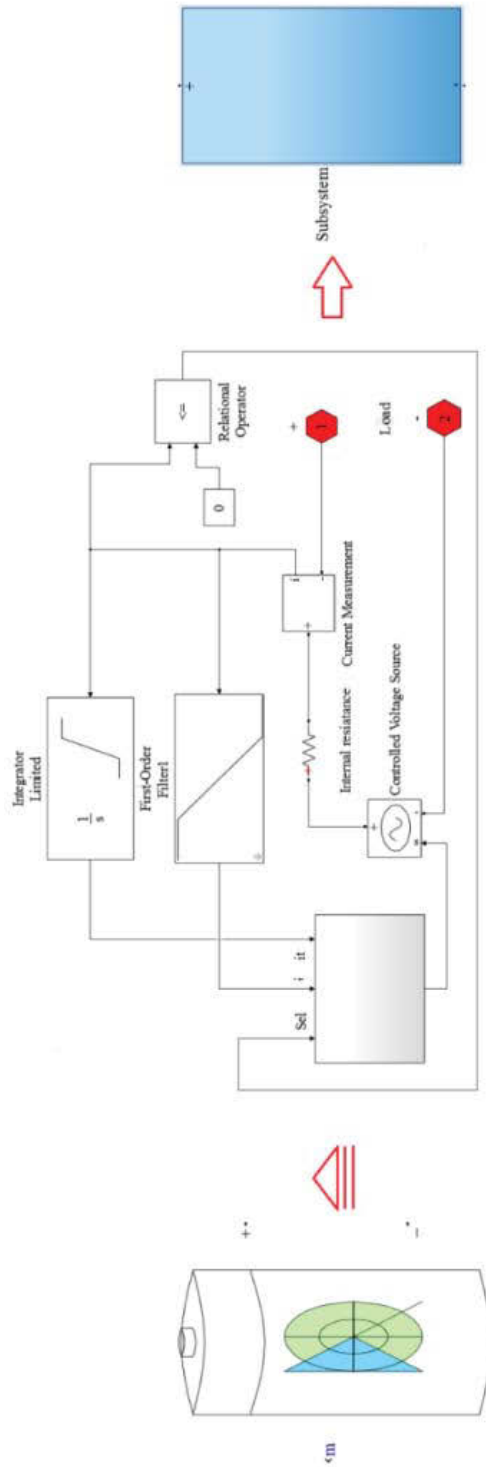


Figure 4.22: Modified battery models in MATLAB simulink

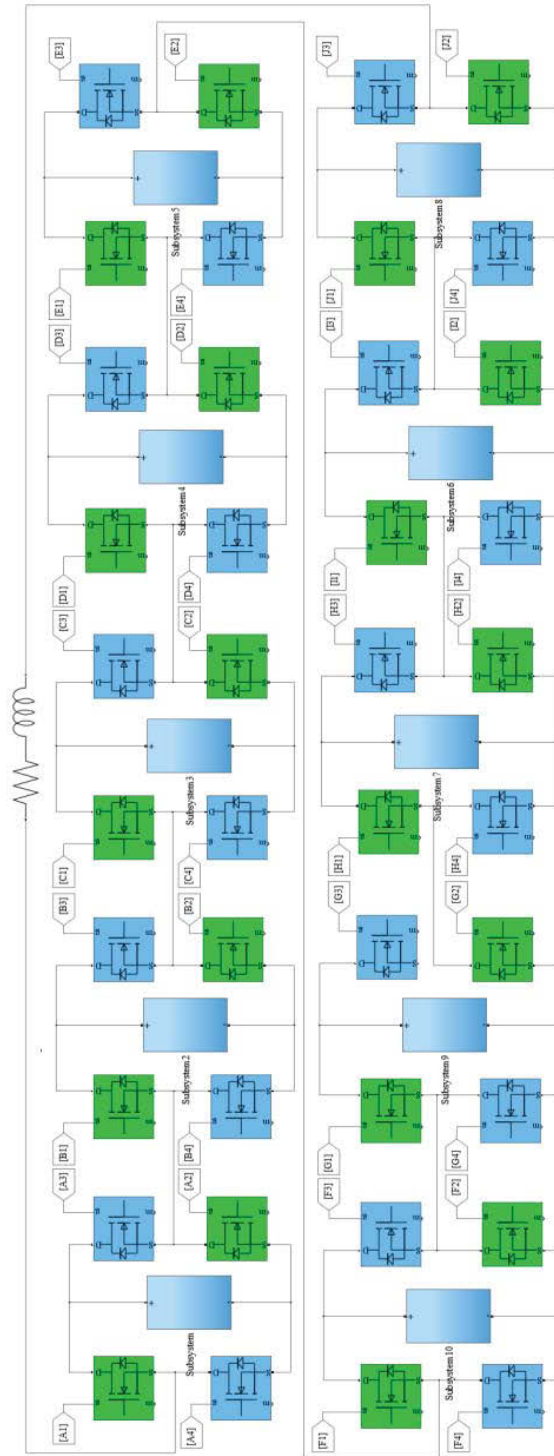


Figure 4.23: Multi-level cascaded H bridge converter with generic battery model



As shown in Figure 4.23, the master block is connected to the slaves and commands the slaves to generate the determined voltage. The code file is attached in the Appendix [A]. In the code file Y1, Y2, Y3, Y4, Y5, Y6, Y7, Y8, Y9, Y10 are the outputs of the master block which is connected to the input of the slave blocks as cell1, cell2, cell3, cell4, cell5, cell6, cell7, cell8, cell9, cell10. Also, in code file “U” is the input of master block or the desired voltage that it is expected the master and slave blocks generate with 10 batteries. The nominal voltage of each battery is 3.7 V. When the desired voltage is not the multiple of 3.7 V, some cells should be on to generate the nearest value to the multiple of 3.7 volts and one cell produce the rest of the voltage by the PWM method. The slave block consists of two inputs as U1 and U2 and four outputs to turn on and off the switches of each bridge. U1 is connected to the master and U2 is connected to the triangular frequency generator which provides the triangular signal with 10 KHz frequency. The switching loss in MOSFET linearly depends on frequency. Higher frequency means higher loss but fewer voltage ripples. In a typical MOSFET application frequency range is from 10 to 20 KHz. Figure 4.24 shows the battery stack output voltage when the desired voltage is changed randomly from -22.2 V to +14 V. Since the PWM method is used for controlling H-bridge switch, the output voltage may have a high harmonic. Figure 4.25 shows the current that extracts from battery-stack.

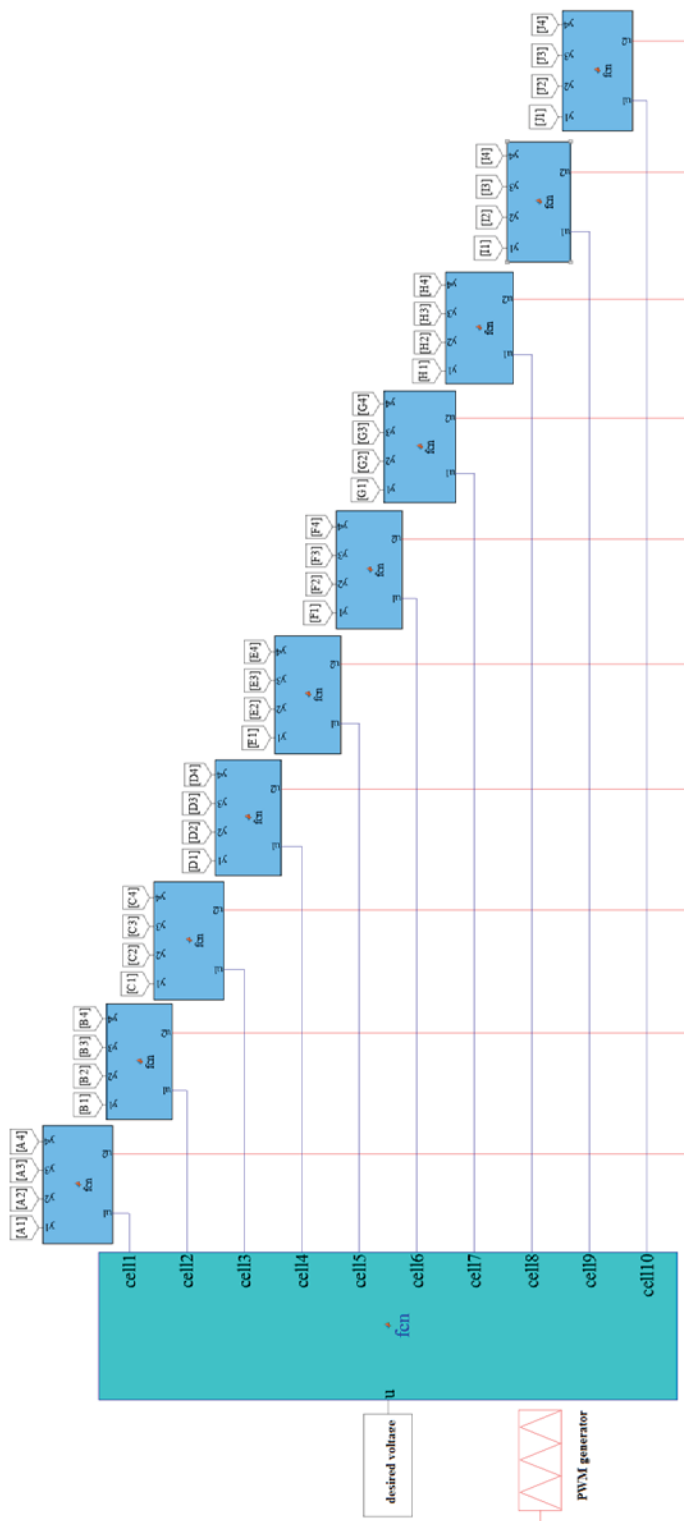


Figure 4.24: Master and slave for multiple-level inverter

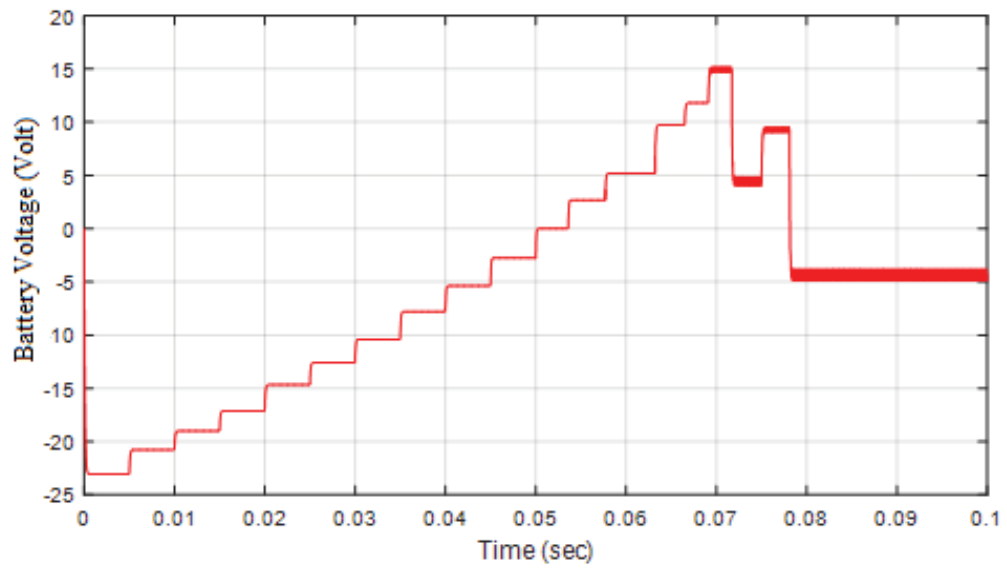


Figure 4.25: Battery stack voltage

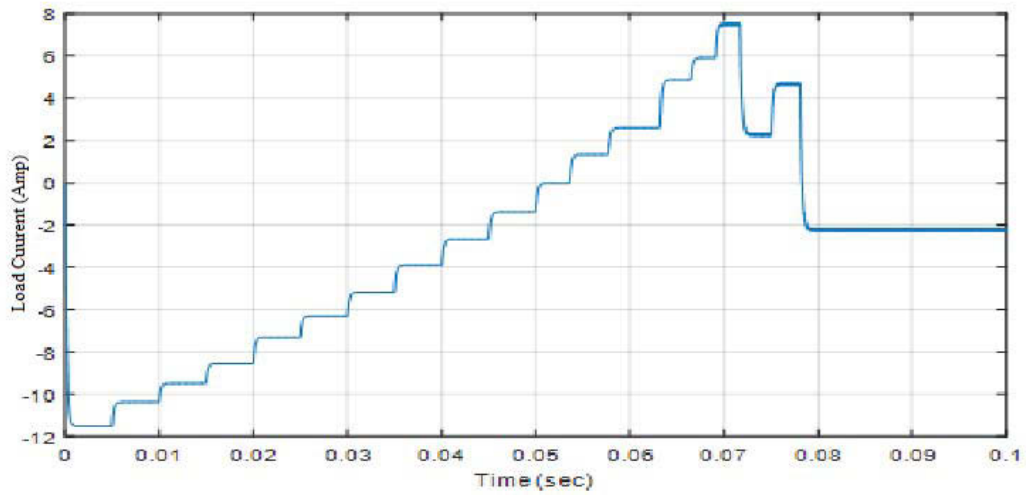


Figure 4.26: Load current

## Chapter 5

### Conclusion and Future Work

In this thesis, the battery stack with ten battery cells is presented. The battery stack is used to control the speed of a DC motor. The battery stack was charged from a grid which converted to DC voltage through an uncontrolled rectifier. Then DC-DC converter was designed to charge the battery stack. The main benefits of the proposed system are summarized as:

- The faulted cell can be keep out of the system for maintenance or replacement without shutting down the output.
- When the battery cell is overcharged, it can be easily bypassed.
- Reducing voltage stress on each cell. In fact in the proposed system each cell in the H-bridge needs to stand only battery cell voltage. This advantage can be more essential in electric vehicle application where inverter switches should meet the battery stack voltage.
- The AC voltage can be obtained by controlling switches to make stair case voltage to go positive and negative peak voltage.

For future research, the following areas can be investigated:

- Generate AC output voltage for induction motor application.
- Analytical model for electric vehicle applications.
- Add temperature effects of battery cell in battery management system.

## Appendix. A

This Appendix shows the codes file used for simulation in this thesis work.

M-file code for Slave block:

```
function [y1,y2,y3,y4] = fcn(u1,u2)
%#codegen

if u1>=0
    if (u1-u2)>0 && u1~=0
        y1=1;y2=1;y3=0;y4=0;
    else
        y1=0;y2=1;y3=0;y4=1;
    end
else
    if (u1-u2)<0
        y1=0;y2=0;y3=1;y4=1;
    else
        y1=0;y2=1;y3=0;y4=1;
    end
end
end
```

M-file code for Master block:

```
function [y1,y2,y3,y4,y5,y6,y7,y8,y9,y10] = fcn(u)
if u== -37;
y1=-3.7;y2=-3.7;y3=-3.7;y4=-3.7;y5=-3.7;y6=-3.7;y7=-3.7;y8=-3.7;y9=-3.7;y10=-3.7;

elseif u== -33.3;
y1=-3.7;y2=-3.7;y3=-3.7;y4=-3.7;y5=-3.7;y6=-3.7;y7=-3.7;y8=-3.7;y9=-3.7;y10=0;

elseif u== -29.6;
y1=-3.7;y2=-3.7;y3=-3.7;y4=-3.7;y5=-3.7;y6=-3.7;y7=-3.7;y8=-3.7;y9=-0;y10=0;

elseif u== -25.9;
y1=-3.7;y2=-3.7;y3=-3.7;y4=-3.7;y5=-3.7;y6=-3.7;y7=-3.7;y8=-0;y9=-0;y10=0;

elseif u== -22.2;
y1=-3.7;y2=-3.7;y3=-3.7;y4=-3.7;y5=-3.7;y6=-3.7;y7=0;y8=-0;y9=-0;y10=0;
```

```

elseif u==-18.5;
    y1=-3.7;y2=-3.7;y3=-3.7;y4=-3.7;y5=-3.7;y6=0;y7=0;y8=-0;y9=-0;y10=0;

elseif u==-14.8;
    y1=-3.7;y2=-3.7;y3=-3.7;y4=-3.7;y5=0;y6=0;y7=0;y8=-0;y9=-0;y10=0;

elseif u==-11.1;
    y1=-3.7;y2=-3.7;y3=-3.7;y4=0;y5=0;y6=0;y7=0;y8=0;y9=0;y10=0;

elseif u==-7.4;
    y1=-3.7;y2=-3.7;y3=0;y4=0;y5=0;y6=0;y7=0;y8=0;y9=0;y10=0;

elseif u==-3.7;
    y1=-3.7;y2=0;y3=0;y4=0;y5=0;y6=0;y7=0;y8=-0;y9=0;y10=0;

elseif floor (u/3.7)==10
    y1=3.7;y2=3.7;y3=3.7;y4=3.7;y5=3.7;y6=3.7;y7=3.7;y8=3.7;y9=3.7;

elseif floor (u/3.7)==-10
    y1=-3.7;y2=-3.7;y3=-3.7;y4=-3.7;y5=-3.7;y6=-3.7;y7=-3.7;y8=-3.7;y9=-3.7;
    y10=rem(u,3.7);

elseif floor (u/3.7)==9
    y1=3.7;y2=3.7;y3=3.7;y4=3.7;y5=3.7;y6=3.7;y7=3.7;y8=3.7;y9=3.7;
    y10=rem(u,3.7);

elseif floor(u/3.7)==-9
    y1=-3.7;y2=-3.7;y3=-3.7;y4=-3.7;y5=-3.7;y6=-3.7;y7=-3.7;y8=-3.7;y9=0;
    y10=rem(u,-3.7);

elseif floor (u/3.7)==8
    y1=3.7;y2=3.7;y3=3.7;y4=3.7;y5=3.7;y6=3.7;y7=3.7;y8=3.7;y9=rem(u,3.7);
    y10=0;

elseif floor (u/3.7)==-8
    y1=-3.7;y2=-3.7;y3=-3.7;y4=-3.7;y5=-3.7;y6=-3.7;y7=-3.7;y8=rem(u,-3.7);
    y9=0;y10=0;

elseif floor (u/3.7)==7
    y1=3.7;y2=3.7;y3=3.7;y4=3.7;y5=3.7;y6=3.7;y7=3.7;y8=rem(u,3.7);y9=0;y10=0;

elseif floor (u/3.7)==-7
    y1=-3.7;y2=-3.7;y3=-3.7;y4=-3.7;y5=-3.7;y6=-3.7;y8=0;y7=rem(u,-3.7);
    y9=0;y10=0;

```

```

elseif floor (u/3.7)==6

y1=3.7;y2=3.7;y3=3.7;y4=3.7;y5=3.7;y6=3.7;y7=rem(u,3.7);y8=0;y9=0;y10=0
;

elseif floor (u/3.7)==-6
    y1=-3.7;y2=-3.7;y3=-3.7;y4=-3.7;y5=-3.7;y7=0;y6=rem(u,-
3.7);y8=0;y9=0;y10=0;

elseif floor (u/3.7)==5

y1=3.7;y2=3.7;y3=3.7;y4=3.7;y5=3.7;y6=rem(u,3.7);y7=0;y8=0;y9=0;y10=0;

elseif floor (u/3.7)==-5
    y1=-3.7;y2=-3.7;y3=-3.7;y4=-3.7;y6=0;y5=rem(u,-
3.7);y7=0;y8=0;y9=0;y10=0;

elseif floor (u/3.7)==4

y1=3.7;y2=3.7;y3=3.7;y4=3.7;y5=rem(u,3.7);y6=0;y7=0;y8=0;y9=0;y10=0;

elseif floor (u/3.7)==-4
    y1=-3.7;y2=-3.7;y3=-3.7;y5=0;y4=rem(u,-
3.7);y6=0;y7=0;y8=0;y9=0;y10=0;

elseif floor(u/3.7)==3
    y1=3.7;y2=3.7;y3=3.7;y4=rem(u,3.7);y5=0;y6=0;y7=0;y8=0;y9=0;y10=0;

elseif floor(u/3.7)==-3
    y1=-3.7;y2=-3.7;y4=0;y3=rem(u,-3.7);
y5=0;y6=0;y7=0;y8=0;y9=0;y10=0;

elseif floor(u/3.7)==2
    y1=3.7;y2=3.7;y3=rem(u,3.7);y4=0; y5=0;y6=0;y7=0;y8=0;y9=0;y10=0;

elseif floor(u/3.7)==-2
    y1=-3.7;y3=0;y2=rem(u,-3.7);y4=0;y5=0;y6=0;y7=0;y8=0;y9=0;y10=0;

elseif floor(u/3.7)==1;
    y1=3.7;y2=rem(u,3.7);y3=0;y4=0; y5=0;y6=0;y7=0;y8=0;y9=0;y10=0;

elseif floor(u/3.7)==-1;
    y2=0;y1=rem(u,-3.7);y3=0;y4=0; y5=0;y6=0;y7=0;y8=0;y9=0;y10=0;
else
    y1=0;y2=0;y3=0;y4=0;y5=0;y6=0;y7=0;y8=0;y9=0;y10=0;
end
end

```

## References

- [1] R. D. Richardson and G. M. McNerney. Wind energy systems, Proceedings of the IEEE, vol. 81, no. 3, pp.378–389, March 1993.
- [2] P. F. Ribeiro, B. K. Johnson, M. L. Crow, A. Arsoy, and Y. Liu. "Energy storage systems for advanced power applications," Proceedings of the IEEE, vol. 89, no. 12, pp.1744–1756, December 2001.
- [3] M. Ehsani, Y. Gao, S. E. Gay, and A. Emadi, Electric vehicles, in Modern electric, hybrid electric, and fuel cell vehicles - fundamentals, theory, and design, Ch 4, Boca Raton, FL: CRC Press, 2005.
- [4] J. Larminie, and J. Lowry, Electric vehicle technology explained, Ch. 2, West Sussex, England: John Wiley & Sons Ltd, 2003.
- [5] Davide Andrea, Battery Management Systems for Large Lithium-Ion Battery Packs, Ch.1, Artech House, 2010.
- [6] A. Shahin, M. Hinaje, J.-P Martin, S. Pierfederici, S. Raël, B. Davat, "High Voltage Ratio DC–DC Converter for Fuel-Cell Applications," Industrial Electronics, IEEE Transactions on , vol.57, no.12, pp.3944–3955, Dec. 2010.
- [7] Mehmet Gultu , batteries and their chemistry ,ch 1.
- [8] N. Watrin, B. Blunier, and A. Miraoui, "Review of adaptive systems for lithium batteries State-of-Charge and State-of-Health estimation," IEEE Transportation Electrification Conference and Expo (ITEC), pp.1-6, 18-20 June 2012.



- [9] L. Gechen, W. Haiying; Y. Zhilong, "New Method for Estimation Modeling of SOC of Battery" WCSE '09. WRI World Congress on , vol.2, pp.387-390, 19-21 May 2009.
- [10] C. A. Swoboda et al., "Development of an Ultrasonic Technique to Measure Specific Gravity in Lead-Acid Battery Electrolyte," IEEE Transactions on Sonics and Ultrasonics, vol. 30, no. 2, pp. 69-77, March 1983.
- [11] A. Keeli and R. K. Sharma, "Optimal use of second life battery for peak load management and improving the life of the battery," Electric Vehicle Conference (IEVC), IEEE International, Greenville, SC, pp. 1-6, 2012.
- [12] Y. Shi, C. Ferone, C. Rao and C.D. Rahn, "Nondestructive forensic pathology of Lead-Acid batteries," American Control Conference (ACC), pp.1350-1355, 27-29 June 2012.
- [13] A. I. Stan, M. Świerczyński, D. I. Stroe, R. Teodorescu and S. J. Andreasen, "Lithium ion battery chemistries from renewable energy storage to automotive and back-up power applications — An overview," International Conference on Optimization of Electrical and Electronic Equipment (OPTIM), Bran, pp. 713-720, 2014.
- [14] Miles, M.H., "Recent advances in lithium battery technology," 23rd Annual Technical Digest in Gallium Arsenide Integrated Circuit (GaAs IC) Symposium, pp.219-222, Oct. 2001.

- [15] K.E Bailey and B.K Powell, "A hybrid electric vehicle powertrain dynamic model," in American Control Conference, Proceedings of the 1995, vol.3, pp.1677-1682, Ch. 2. Jun 1995.
- [16] O. Tremblay, L.A. Dessaint, A.I. Dekkiche, "A Generic Battery Model for the Dynamic Simulation of Hybrid Electric Vehicles," Vehicle Power and Propulsion Conference VPPC, IEEE pp.284-289, Sept. 2007.
- [17] H. Hongwen, R. Xiong, Z. Xiaowei, S. Fengchun, F. JinXin, "State-of-Charge Estimation of the Lithium-Ion Battery Using an Adaptive Extended Kalman Filter Based on an Improved Thevenin Model," IEEE Transactions on Vehicular Technology, vol.60, no.4, pp.1461-1469, May 2011.
- [18] J.Asumadu, M. Haque, H. Vogel and C. Willards, "Precision battery management system. In Instrumentation and measurement technology conference". Symposium conducted at the meeting of IEEE, Ottawa, Ontario, May 2005.
- [19] K. Karnjanapiboon, K. Jirasereeamornkul, and V. Monyakul, "High efficiency battery management system for serially connected battery string," IEEE international symposium on industrial electronics. Korea, July 2009.
- [20] N. Kutku, and M. Divan, "Dynamic equalization techniques for series battery stacks. In Telecommunications energy conference," Symposium conducted at the meeting of INTELEC, Boston, MA. 1996.
- [21] C. Bonglio, and W. Roessler "A cost optimized battery management system with active cell balancing for lithium ion battery stacks," Vehicle Power and Propulsion Conference, pp. 304-309, 2009.

- [22] A. Baughman, & M. Ferdowsi "Double-tiered switched-capacitor battery charge equalization technique," IEEE Transactions on Industrial Electronics, vol. 55, no. 6, pp.2277-2285, 2008.
- [23] G. Zheng, J. Zhao, "Implementation of a novel digitally- controlled lead-acid battery management system," IEEE Intelligent computing and intelligent systems, Shanghai, China, November 2009.
- [24] S. Moore, P. Schneider, "A review of cell equalization methods for lithium ion and lithium polymer battery systems" SAE World Congress, Detroit, MI, 2001.
- [25] Ned Mohan, "First course on power electronics and drives", 3<sup>rd</sup> Edition, 2003.